Quaternary Science Reviews 243 (2020) 106484

Contents lists available at ScienceDirect

Quaternary Science Reviews

journal homepage: www.elsevier.com/locate/quascirev

Summer temperature development 18,000–14,000 cal. BP recorded by a new chironomid record from Burgäschisee, Swiss Plateau

Alexander Bolland [a, *], Fabian Rey [a, b], Erika Gobet [b], Willy Tinner [b], Oliver Heiri [a]

[a] Geoecology, Department of Environmental Sciences, University of Basel, Klingelbergstrasse 27, CH-4056, Basel, Switzerland
[b] Institute of Plant Sciences and Oeschger Centre for Climate Change Research, University of Bern, Altenbergrain 21, CH-3013, Bern, Switzerland

ARTICLE INFO

Article history:
Received 1 April 2020
Received in revised form
3 July 2020
Accepted 10 July 2020
Available online xxx

Keywords:
Chironomids
Palaeoecology
Palaeolimate
Temperature
Lateglacial
Afforestation

ABSTRACT

The termination of the Last Ice Age after the Last Glacial maximum (LGM) represents a dynamic period in the history of the circum-north Atlantic region. So far, there are few reliably dated climatic reconstructions covering the Lateglacial period prior to 14,700 cal. BP in Central and Northern Europe. We present a new chironomid record for the period 18,000–14,000 cal. BP, from Burgäschisee, Switzerland. Chironomid assemblages immediately following glacier retreat were dominated by taxa indicative of cold, oligotrophic conditions such as *Sergentia coracina* -type and *Micropsectra radialis* -type. A gradual transition to assemblages with moderate abundances of taxa indicative of warmer climatic conditions such as *Dicrotendipes nevosus* -type and *Tanytarsus glabrescens* -type started after ca. 16,100 cal. BP. This initial and gradual chironomid assemblage shift culminated in a more pronounced and rapid inferred temperature change at the Oldest Dryas/Bølling transition at ca. 14,700 cal. BP, where further types indicative of warm conditions such as *Tanytarsus lactescens* -type first occurred and replaced chironomids indicative of colder conditions such as *Paracladius* and *Protanypus*. We estimated past July air temperature changes from the chironomid assemblages by applying to the record a chironomid-temperature transfer function that is based on chironomid distribution data from 274 lakes in Switzerland and Norway. The resulting reconstruction, which features a sample-specific root mean square error of prediction of 1.36–1.46 °C, indicates temperatures around 9 °C at the beginning of the record. An initial gradual warming phase initiating at ca. 16,100 cal. BP is recorded reaching values around 10 °C for the period 16,100–15,500 cal. BP. Temperatures continue to increase reaching values around 12 °C for the period preceding the Bølling warming, when temperatures rose rapidly to values around 15 °C. The early temperature rise to values of 10–12 °C prior to the Bølling warming agrees with widespread vegetation changes recently reported for this region based on palaeobotanical analyses, which indicate a shift from herbaceous tundra to shrub tundra with low density tree birch stands with open canopies. Together, these results suggest an earlier Lateglacial temperature increase in southwest Central Europe than expected based on earlier palaeobotanical reconstructions, although with a less pronounced warming than has been reported for ca. 16,000 cal. BP from south of the Alps. This early Lateglacial warming agrees with glacier reconstructions which suggest several step-wise reductions of glacier extent in this period as well as with evidence from other palaeotemperature reconstructions and suggests that not only Southern Europe but significant parts of Europe north of the Alps may have been characterized by early Lateglacial warming well before the rapid warming at ca. 14,700 cal. BP.

1. Introduction

The end of the last ice age (termination I) represents one of the most dynamic and widespread natural environmental and climatic regime shifts in the past 100 ka. Termination I coincided with increasing northern hemisphere insolation, rising sea levels and massive freshwater inputs into the global oceans following the Last Glacial Maximum (LGM: ca. 26,500 - 19,000 years ago), during which time relative sea level was ca. 130 m lower than it is today (Clark et al., 2009). Between 19,000 and 17,000 years ago increasing temperatures are registered for many parts of the globe, in accordance with rising northern hemisphere insolation values (He et al.,

* Corresponding author.
E-mail address: alexanderwilliam.bolland@unibas.ch (A. Bolland).

https://doi.org/10.1016/j.quascirev.2020.106484

2013). Increases in greenhouse gas concentrations recorded in ice cores during this period are generally interpreted as the result of a complex interplay between changes in overturning circulation in the Southern Ocean and North Atlantic, sea ice extent, atmospheric circulation and biological activity associated with these mechanisms following initial warming (e.g. Petit et al., 1999; Fischer et al., 2008; Marcott et al., 2014). Water isotope records from Antarctic ice cores indicate an increase in southern hemisphere temperatures starting as early as 20,000–18,000 years ago (NAIS Divide Members, 2013).

Evidence for a long-term temperature increase during termination I from the southern hemisphere and at the global scale contrasts to the situation in the northern North Atlantic region where environmental changes were particularly dynamic. Rapid, high volume variations in freshwater input into the North Atlantic have been considered as potential causes for reduced Atlantic Meridional Overturning Circulation (AMOC; Clark et al., 2012; Stern and Lisiecki, 2013) during large parts of this interval, reducing transport of warm waters from southern latitudes northwards (e.g. McManus et al., 2004) and maintaining low North Atlantic (Liu et al., 2009; Mojtahid et al., 2017) sea surface temperatures. As a consequence, it is generally considered that cold conditions prevailed in large sections of the northern North Atlantic region until the abrupt increase in AMOC and associated abrupt warming at the transition to the Lateglacial (Bølling/Allerød) interstadial ca. 14,700 years ago (e.g. Clark et al., 2012; Rasmussen et al., 2014).

The abrupt changes in the North Atlantic Ocean are reflected in vegetation reconstructions that, in the circum-North Atlantic region, are the primary information source for understanding climate dynamics on the continents during termination I. For Southern Europe comprehensive vegetation reconstructions are available for the entirety of the LGM and Termination I, both regionally from marine cores (Fletcher and Goñi, 2008; Fletcher et al., 2010) and more locally in terrestrial records from sites that were never glaciated (e.g. Pons and Reille, 1988; Watts et al., 1996; Allen et al., 2000; Tzedakis et al., 2002; Kaltenrieder et al., 2009). In contrast, most well dated Northern and Central European sites, including sites in France and Northern Spain, have chronological constraints of ca. 14,500–18,000 calibrated radiocarbon years BP (cal. BP) for their lowermost dates (e.g. Magny et al., 2006; Wehrli et al., 2007; Millet et al., 2012). Many of these sites were covered by ice during the LGM and early parts of Termination I (e.g. Hughes et al., 2016) and in large sections of Central and Northwest Europe that were not ice covered a dry climate prevailed (e.g. Hoek and Bohncke, 2002), limiting the number of lakes and therefore also of limnological records. Until now, few Northern and Central European records exist which are reliably dated and describe vegetational assemblages prior to the onset of the Bølling/Allerød interstadial ca. 14,700 cal. BP (Lotter et al., 1999; Duprat-Oualid et al., 2017; Rey et al., 2017; 2020). As a consequence, it remains difficult to constrain when temperatures first started to rise after the LGM on mainland Europe and how far in the European interior the climatic development followed that of the North Atlantic during the early termination.

Based on the available evidence, persistence of a cold tundra and/or steppic environment has been assumed for Central Europe following the LGM until the regional reforestation at the onset of the Bølling (e.g: Lotter et al., 1992; Wehrli et al., 2007). However, new evidence from ^{14}C dated lake sediments from the Northern Swiss lowlands indicates a clear transition from herb tundra into a more diverse herb/shrub tundra as early as 16,000 cal. BP (Rey et al., 2017; 2020). Recent pollen-morphological differentiation of tree and shrub birches allowed to track the expansion of first tree *Betula* stands at around 16,000 cal BP, a vegetational pattern that was unknown before (Rey et al., 2017; 2020). The implication is the possibility of warming ca. 1300 years prior to the rapid warming phase at the onset to the Bølling period around 14,700 cal. BP. Afforestation prior to the Bølling onset has previously been observed in pollen records from the western Mediterranean region (Fletcher et al., 2010) and both pollen- and chironomid-based temperature reconstructions have indicated early warming at Lago di Origlio (Southern Switzerland) chronologically placed at the same time as the new evidence from the Northern Swiss lowlands (Tinner and Vescovi, 2005; Samartin et al., 2012). There are however no well-dated, vegetation-independent terrestrial temperature records from north of the Alps to corroborate this hypothesized early temperature increase. Since vegetation development in a tundra and/or steppe environment is not only determined by temperature, but can potentially also be strongly influenced by moisture changes (Tinner, 2007; Samartin et al., 2017), such independent temperature reconstructions would be crucial for confirming that these vegetation changes really were the direct consequences of warmer temperatures during the Early Lateglacial period.

Chironomid analysis is an excellent tool for reconstructing past summer temperature changes because of the strong relationship between chironomid distribution and July air temperatures (Brooks and Birks, 2001; Heiri and Lotter, 2005; Eggermont and Heiri, 2012). This relationship has allowed the production of modern calibration training sets which can be used to develop quantitative chironomid-based temperature inference models to reconstruct palaeotemperature development from lake sediment records (Brooks et al., 2006). There are many examples of chironomids being used to reconstruct Lateglacial temperature changes in Switzerland (e.g. Heiri and Lotter, 2005; Ilyashuk et al., 2009; Samartin et al., 2012) and other regions of Central, Western and Northern Europe (e.g. Brooks and Birks, 2000; Heiri and Millet, 2005; Heiri et al., 2007a; Watson et al., 2010; Millet et al., 2012; Birks et al., 2014) as well as Southern Europe (Heiri et al., 2007b; Larocque and Finsinger, 2008; Samartin et al., 2017). However, as with the aforementioned pollen analysis, only very few chironomid-based temperature reconstructions from Europe, such as those described by Millet et al. (2012, Western Pyrenees, France) and Samartin et al. (2012, Ticino, Southern Switzerland), cover the crucial time interval before the beginning of the Lateglacial Interstadial ca. 14,700 cal. BP and are supported by independent chronological constraints for this older section of the Lateglacial period. Up to the present, no such chironomid-based temperature reconstructions are available for the Central European lowlands north of the Alps.

Here, we present a new chironomid record from Burgäschisee in the Western Swiss Plateau covering the Early Lateglacial period from ca. 18,300 to 14,000 cal. BP. In-lake environmental changes inferred from the record are discussed in relation to the taxonomic turnover in chironomid assemblages. Furthermore, we develop a new quantitative, chironomid-based summer temperature reconstruction from the record which covers the full Early Lateglacial period since lake formation following local deglaciation. Previous pollen analyses from the same sediment record have revealed evidence for a pre-Bølling vegetation change from steppe to shrub tundra, suggesting increasing temperatures in this region from ca. 16,000 cal. BP onwards (Rey et al., 2017). Therefore, the new temperature record can be directly compared to local vegetation changes to assess whether this independent palaeotemperature evidence really supports that increasing summer temperatures were responsible for local vegetation compositional turnover around 16,000 cal. BP. Finally, we discuss the implications of our results for constraining palaeotemperature development in Switzerland and early Lateglacial temperature development on continental Europe.

2. Material and methods

2.1. Site description

Burgäschisee is a small kettle hole lake, formed following the retreat of the Rhone glacier westwards across the Swiss plateau, situated between the Jura Mountains and the Alps (Fig. 1; 47°10′8.5″N, 7°40′5.9″E) at 465 m a.s.l. (Fig. 1). A section of ice remaining after glacier retreat was subsequently surrounded and possibly covered by sediments after which the ice melted, leaving a depression and forming the lake (Guthruf et al., 1999). Today, Burgäschisee is eutrophic, has a 23 ha surface area, maximum depth of 31 m and a catchment of 319 ha (Guthruf et al., 1999). Four inflows feed the lake from the Southwest and a single outflow drains the lake to the North (Müller-Beck, 2005). The lake level was lowered by 2 m in 1943 in order to drain wetlands for agricultural use (Arn, 1945). The outflow of the lake has been artificially modified to release deep, hypolimnetic waters since 1977 to reduce the nutrient loading of the lake and improve the water quality (Ambühl and Stumm, 1984).

Annual rainfall is ca. 1100 mm (data from Koppigen 1981–2010 climate normals), ca. 6 km from Burgäschisee (MeteoSwiss, 2020), and the wettest months occur May through August with more than 100 mm of precipitation per month. July is the warmest month reaching 18.6 °C on average while the annual average temperature is 9.1 °C.

2.2. Coring

Two field campaigns were carried out at Burgäschisee in 2009 and 2014. Three parallel cores (Burg A-C) were retrieved in 2009 using a UWITEC piston corer with a diameter of 60 mm at the deepest point of the lake reaching a coring depth of 15 m. A further core, Burg I, was retrieved in 2014 to create a master sequence using lithostratigraphic markers for the core correlation (Rey et al., 2017). The core section analysed in the present study consists of silt (1037-846 cm) and fine detritus gyttja which is partially laminated (846-826 cm). A detailed description of the sedimentology is provided in Rey et al. (2017).

2.3. Dating and vegetation history

The Burgäschisee sediment record is dated by a total of 16 radiocarbon dates, 4 of which are used to date the section presented here as described in Rey et al. (2017). ^{14}C samples were analysed at the Laboratory for the Analysis of Radiocarbon at Bern University, the Laboratory of Ion Beam Physics at ETH Zurich, and the Poznan Radiocarbon Laboratory using Accelerator Mass Spectrometry (AMS). Calib 7.1 (Stuiver and Reimer, 1993) was used to calibrate the radiocarbon dates using the IntCal13 calibration curve (Reimer et al., 2013). An age-depth relationship for the entire Burgäschisee sequence is available based on the program clam 2.2 (Blaauw, 2010) as described in Rey et al. (2017).

Lateglacial sections of this age model were characterized by relatively large uncertainties (Fig. 2). For the present study, we

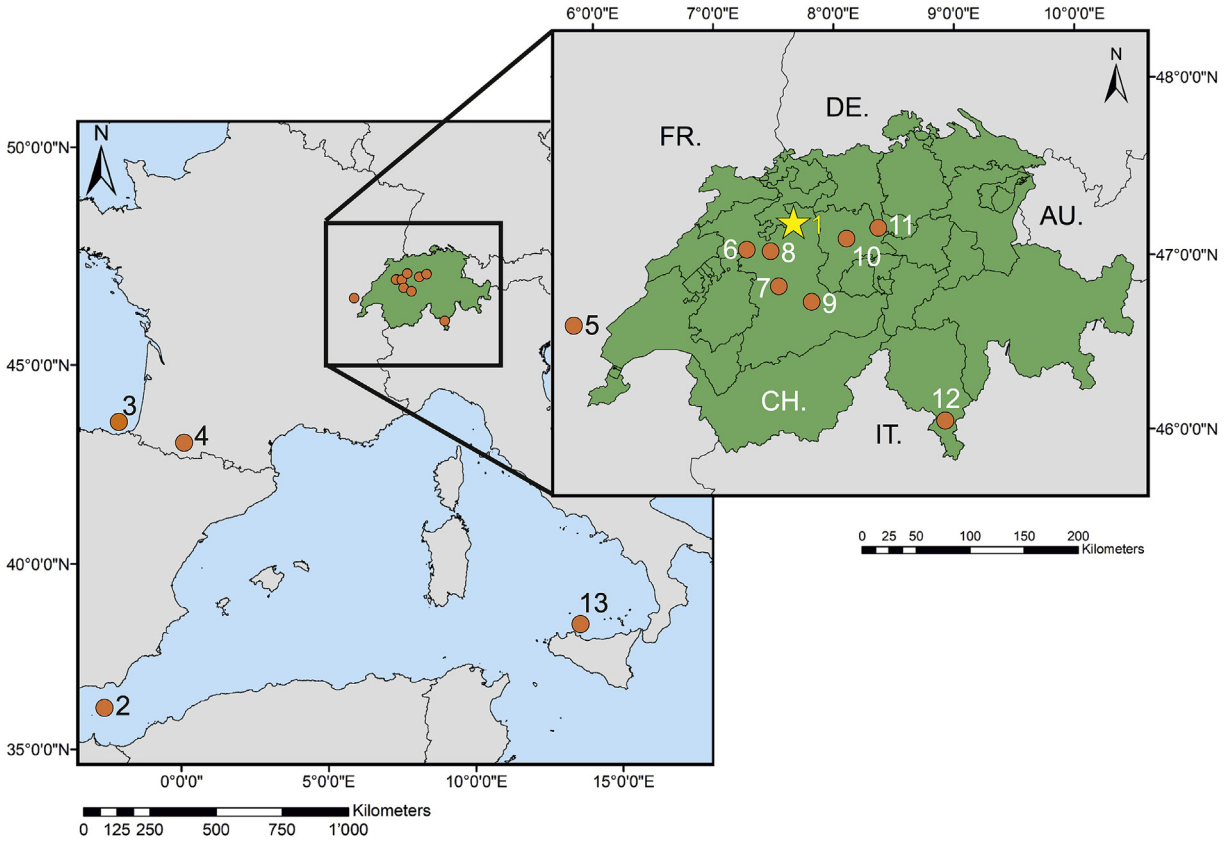

Fig. 1. Location of Burgäschisee in Switzerland (green area) and of other records discussed in text. 1: Burgäschisee (Rey et al., 2017; This study); 2: Core MD95-2043, Alboran Sea (Cacho et al., 2001; Fletcher et al., 2010); 3: Core KS04-16, Bay of Biscay (Martínez-García et al., 2015); 4: Ech Palaeolake (Millet et al., 2012); 5: Lac Lautrey (Heiri and Millet, 2005); 6: Lobsigensee (Elias and Wilkinson, 1983); 7: Gerzensee (Brooks and Heiri, 2013; Lotter et al., 2012; Ammann et al., 2013; van Raden et al., 2013); 8: Moossee (Rey et al., 2020); 9: Sieben Hengste (Luetscher et al., 2015); 10: Soppensee (Lotter, 1999); 11: Rotsee (Lotter and Zbinden, 1989); 12: Lago di Origlio (Samartin et al., 2012) and 13: Core BS79-38, Tyrrhenian Sea (Cacho et al., 2001). (For interpretation of the references to colour in this figure legend, the reader is referred to the Web version of this article.)

therefore also explored an alternative age model using other available age estimates for major vegetation changes on the Swiss Plateau between 13,800 and 14,700 cal. BP. Several studies have shown that major shifts in vegetation such as the reforestation and increase in *Juniperus* at the Oldest Dryas to Bølling transition or the increase in *Pinus* at the Older Dryas cold oscillation happened at the same time as pronounced changes in climatic conditions on the Swiss Plateau as apparent in lake marl $\delta^{18}O$ records, therefore indicating that these vegetation shifts happened synchronously across the Swiss Plateau (Lotter et al., 1992; Eicher and Siegenthaler, 1976), at least at the multidecadal to centennial scale relevant for the present study. The ages of prominent Lateglacial vegetation changes in the Burgäschisee record as dated in other Lateglacial sediment sequences on the Swiss Plateau therefore provide further age constraints for the record.

Three strong palynostratigraphical age markers were identified which correspond to distinct vegetative transitions in the Burgäschisee pollen stratigraphy (Table 1) and were correlated to the well-dated Gerzensee pollen stratigraphy (Ammann et al., 2013), a record that is representative of regional vegetation development across the Western Swiss lowlands for this study period. Ages of these vegetation changes in the Gerzensee record show an excellent agreement with ages as assessed in the ^{14}C dated pollen record from Moossee, 22 km southwest of Burgäschisee, situated at almost identical altitude (512 m asl; Fig. 2). Furthermore, the inferred age of the increase in lake marl $\delta^{18}O$ record of Gerzensee at the beginning of the Bølling at 14,685–14,590 cal. BP, which coincides with the increase in *Juniperus* and reforestation of the Swiss Plateau, shows an excellent agreement with the pronounced increase in precipitation $\delta^{18}O$ inferred for 14,658 ± 40 cal. BP (Luetscher et al., 2015) based on the U/Th dated speleothem from Sieben Hengste (46 km from Burgäschisee, 22 km from Gerzensee), supporting the estimated age for this vegetation change on the Swiss Plateau.

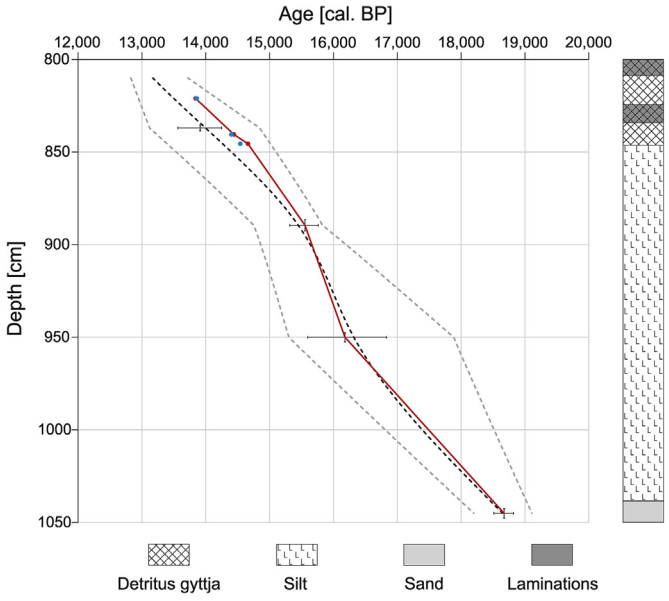

Fig. 2. Lithology and age depth model of the oldest sections of the Burgäschisee record. Black crosses indicate the ^{14}C dates used by Rey et al. (2017, Table 1), dotted black and grey lines the original age-depth relationship described in this study as well as the associated 95% error estimates. Red circles represent the age of palynostratigraphical tie points in the Burgäschisee record as dated in the Gerzensee pollen record (Ammann et al., 2013, Table 1), blue circles age estimates for these tie points as dated in the Moossee pollen record (Rey et al., 2020). Age estimates for Lateglacial section of the Moossee record are based on 6 AMS ^{14}C dates and the Gerzensee record is dated based on the correlation of lake marl $\delta^{18}O$ values with the NGRIP Greenland ice core $\delta^{18}O$ record (age uncertainties for the latter record are estimated as 169–186 years for this interval (maximum counting error); Rasmussen et al., 2006). Moossee and Gerzensee are both situated on the Swiss Plateau in close proximity to Burgäschisee (22 and 39 km distant from the lake, respectively). The red line indicates the revised age model for the Burgäschisee record based on linear interpolation between the radiocarbon dates in the lower part of the record and the palynological tie points in the upper section (see text for details). (For interpretation of the references to colour in this figure legend, the reader is referred to the Web version of this article.)

These pollen-inferred ages suggest that one of the ^{14}C ages (835.5–838.5 cm, 13,997 cal yr BP) is slightly younger than expected based on the pollen based age estimates (Fig. 2). When comparing the Burgäschisee chironomid record with other palaeoclimate records, we therefore use a revised age-depth model based on linear interpolation between median calibrated ^{14}C ages for the older part of the record and the three pollen-inferred ages for the upper part of the sequence between 849 and 823 cm sediment depth (Table 1, Fig. 2). This revised age depth relationship is fully within the chronological error associated with the original age depth model of Rey et al. (2017) (Fig. 2). For information we also provide the figures comparing chironomid-inferred temperatures with other palaeoenvironmental reconstructions discussed in our study (Figs. 5 and 6) on the original age scale presented by Rey et al. (2017) in the online supplementary information.

The main traits of vegetation history at Burgäschisee over the past 18,700 years are presented in Rey et al. (2017). The pollen data suggest open steppe/tundra vegetation (Rey et al., 2020) shortly after deglaciation at ca. 19,200 cal BP (Ivy-Ochs et al., 2004), with the presence of some shrubs including *Betula nana* and *Juniperus*. Herb dominated tundra ecosystems persisted until ca. 16,000 cal BP when there was a marked increase of tree *Betula*, *Betula nana* and other shrubs pointing to the spread of shrub tundra and tree stands (Rey et al., 2017). However, the prevailing presence of herbaceous pollen values (>60% including abundant *Artemisia* and *Helianthemum*) shows that steppic environments persisted and still dominated the vegetation. The Oldest Dryas/Bølling transition was characterized by afforestation within the catchment of Burgäschisee with a short term mass expansion of shrubs (*Juniperus* pollen >60%) during early sections of the Bølling warming period (Ammann et al., 2013) followed by a sharp rise in tree *Betula* pollen which suggests the formation of birch forests. At the same time, the organic content of the sediment rises sharply, showing increased organic productivity in the lake (Rey et al., 2017).

2.4. Sampling and analysis of fossil chironomids and other aquatic invertebrates

Samples were taken every ca. 4–6 cm using 2–20 cm^3 of wet sediment per sample. A total of 36 samples were analysed at absolute sediment depths between 826 and 1032 cm. The samples were left in room temperature in 10% KOH for 6 h and sieved over a 100 μm sieve. Chironomid head capsules as well as other chitinous aquatic invertebrate remains were picked from other sieve residue in a Bogorov tray under a stereomicroscope (30–50× magnification), dried on coverslips and mounted on microscope slides in Euparal before being identified at 40–100× magnification using a compound microscope. A minimum head capsule count of 80 was aimed for to ensure that more than the recommended 50 head capsules were found per sample (Heiri and Lotter, 2001; Quinlan and Smol, 2001). Two samples nevertheless resulted in less than the 50 head capsules (sample depths 836 and 888 cm contained 47 and 42 head capsules, respectively). Head capsules with a complete mentum or greater than half a mentum were counted as one specimen, head capsules with half a mentum were counted as half a specimen and head capsules with less than half a mentum were disregarded.

Taxonomic identification followed Wiederholm (1983), Schmid

Table 1
Radiocarbon dates and calibrated ages from the Burgäschisee record. ^{14}C dates are from Rey et al. (2017). Ages are calibrated with the program Calib 7.1 (Stuiver and Reimer, 1993) and the IntCal13 calibration curve (Reimer et al., 2013). Pollen-inferred ages represent the age of these landscape scale vegetation changes as assessed in the sediments of Gerzensee, 58 km from Burgäschisee (van Raden et al., 2013). Radiocarbon analysis was conducted at Laboratory of Ion Beam Physics, ETH Zurich, Switzerland[a]; Laboratory for the Analysis of Radiocarbon, Bern University, Switzerland[b] and Poznan Radiocarbon Laboratory, Poland[c].

Lab. code	Depth (cm)	Material/age marker	^{14}C age (BP)	Age (cal BP)	Age 2σ range (cal BP)	Age used in age/depth relationship (cal BP)
	818.5–823.5	Palynological stratigraphy (*Betula* phase to Allerød Pine and *Betula* phase)		13,840		13,840
BE-2552.1.1[b]	835.5–838.5	*Betula* fruits, fruit scale	12,050 ± 130	13,997	13,579–14,414	Not used
	838.5–842.5	Palynological stratigraphy (*Juniperus* peak to *Betula* phase)		14,440		14,440
	842.5–848.5	Palynological stratigraphy (Oldest Dryas to *Juniperus* peak)		14,660		14,660
ETH-43949[a]	886.5–892.5	*Betula nana* fruit scales, fruits; periderm deciduous, leaf fragments deciduous, bud scales deciduous, twiglet, bark	13,000 ± 50	15,540	15,316–15,764	15,540
BE-2553.1.1[b]	947.5–952.5	Twiglet	13,440 ± 200	16,140	15,512–16,767	16,140
Poz-60131[c]	1042.5–1047.5	Twiglet	15,400 ± 70	18,665	18,512–18,817	18,665

(1993), Brooks et al. (2007), and Anderson et al. (2013). For graphical and statistical interpretation, specimens that could not be identified to the highest taxonomic resolution (e.g. due to missing mouthparts) were assigned to categories based on the ratio of identified specimens within the sample. For these calculations, taxa which could not be assigned beyond subfamily/tribe level (i.e. unidentified Chironomidae, Chironomini, Tanytarsini, Orthocladiinae) were excluded.

2.5. Zonation and ordination analyses

Zonations were derived using the clustering algorithm CONISS (Grimm, 1987) and zonations were compared with a Broken Stick Model to assess the statistical significance of the zonal boundaries (Bennett, 1996). CONISS was calculated with Rioja (Juggins, 2017) and Vegan (Oksanen et al., 2007) packages using R studio version 1.1.463 (RStudio Team, 2015).

Major changes in chironomid assemblage composition were summarized with a Detrended Correspondence Analysis (DCA) using CANOCO 5.0 (ter Braak and Smilauer, 2018) and square root transformed percentage data. Changes were summarized as DCA axis 1 values expressed in standard deviation (SD) units, the length of DCA axis 1 was 2.5 SD. Changes in in-lake nutrient concentrations and affected variables such as algal productivity or oxygen concentrations in the lake can have a major influence on lacustrine chironomid assemblages (e.g. Brodersen and Quinlan, 2006). We used direct gradient analysis of a dataset representing chironomid assemblage composition in 28 deep and stratified lakes across Europe (41.7–68.4°N; Verbruggen et al., 2011) to explore the extent that changes in fossil chironomid assemblages at Burgäschisee were typical for shifts to more nutrient-rich (eutrophic) or nutrient-poor (oligotrophic) conditions. We analysed the data from these 28 lakes with Detrended Canonical Correspondence Analysis (DCCA) using total phosphorus (TP) concentrations at these sites as only constraining variable. As a consequence, DCCA axis 1 is constrained to represent changes in modern chironomid assemblages related to between-site differences in TP values. Fossil samples from Burgäschisee were entered in this analysis as passive samples, and variations in their DCCA axis 1 values can therefore be interpreted as indicating whether past assemblage changes were towards assemblages more typical for nutrient-rich or nutrient-poor lakes in the calibration dataset. TP values are used for constraining DCCA since phosphorus is typically the limiting element for algal growth in lakes. The applied dataset includes lakes from Lapland to Southern Italy (Verbruggen et al., 2011), and TP values correlate to some extent with both air temperatures and hypolimnetic oxygen availability at these study lakes. All of these lakes are deep (22–370 (mean 100) m water depth), stratified systems, however, in which larval chironomid assemblages are largely decoupled from the direct effects of air and surface water temperatures. Changes in DCCA axis 1 are therefore considered to mainly reflect changes in respect to different nutrient conditions at the studied lakes and not the influence of temperature on chironomid assemblages, in contrast to the shallower lakes that were used to develop the chironomid-temperature transfer function for reconstruction of past summer temperatures from the Burgäschisee chironomid assemblages (see section 2.6 below). DCCA was calculated on square-root transformed percentage data using the program CANOCO 4.5 (Leps and Smilauer, 2003).

2.6. Temperature reconstruction

A chironomid-temperature inference model based on the Swiss-Norwegian calibration dataset (Heiri et al., 2011) was used

to develop quantitative temperature estimates from fossil chironomid assemblages in Burgäschisee. The model is based on samples from 274 lakes throughout Switzerland and Norway, describing distribution data of 154 chironomid taxa and covering a July temperature gradient of 3.5–18.4 °C. In contrast to the dataset used for exploring chironomid assemblage changes typical for changes in nutrient availability (see section 2.5.) this dataset consisted of considerably shallower lakes (mean 10 m, 5–95% percentile range 1.3–26 m, range 0.5–77 m maximum water depth) for which strong relationships between chironomid assemblage composition and summer temperature values have been demonstrated (e.g. Eggermont and Heiri, 2012) and that perform well for development of chironomid-temperature transfer functions.

A two component weighted averaging partial least squares model (WAPLS; ter Braak and Juggins, 1993; ter Braak et al., 1993) was used to produce the temperature reconstruction, percentages were square root transformed before calculations. Of the 64 chironomid morphotypes originally identified in the Burgäschisee record, some had to be amalgamated for the temperature reconstruction resulting in 53 types in total. The resulting inference model featured a cross validated (bootstrapped) root mean square error of prediction of 1.40 °C and a r^2 value of 0.87 between observed mean July air temperature values and those inferred based on chironomid assemblages in the modern calibration data. WA-PLS was calculated using the program C2 version 1.77 (Juggins, 2007).

2.7. Reconstruction error and diagnostic statistics

Sample specific error estimates were calculated for each reconstructed temperature in the Burgäschisee record using bootstrapping (9999 cycles, Birks et al., 1990). Fossil sample were compared with samples in the calibration dataset to identify assemblages with “no good” and “no close” analogues using squared chi-square distance (Birks et al., 1990). The 5th and 2nd percentiles of all distances within the modern calibration data samples were used as thresholds to identify fossil samples without good and close analogues, respectively (Birks, 1990; Toth et al., 2015). Furthermore, goodness-of-fit statistics (Birks et al., 1990, 2010) were used to identify samples with an unusual composition, which might indicate that variables other than temperature were exerting a dominating influence on assemblages. Fossil assemblages were analysed as passive samples in a Canonical Correspondence Analysis (CCA) of the modern calibration dataset with mean July air temperature as only constraining variable. Residual distances to CCA axis 1 were considered to represent “goodness-of-fit” with temperature, and thresholds of the 90th and 95th percentile of residual distances of modern calibration dataset samples to axis 1 were used to identify samples with a “poor” or “very poor” fit with temperature (Birks, 1990; Toth et al., 2015). Finally, for each sample we examined the percentage of identified chironomids that were not represented in the calibration dataset, as well as the percentage of identified chironomids that were rare in the calibration data (represented by a Hill’s N2 lower than 5; Heiri et al., 2003). Analogue statistics were calculated with the program C2 version 1.77 (Juggins, 2007) and CCA with CANOCO 4.5 (Leps and Smilauer, 2003).

3. Results

3.1. The Burgäschisee chironomid record

A total of 56 chironomid taxa were identified from 36 samples. Downcore changes in the Burgäschisee chironomid record mostly showed gradual changes in assemblages with two periods of accelerated turnover which have been identified as statistically significant breaks by CONISS zonation. The zones identified by CONISS (Burg 1 through Burg 3) are used here for describing chironomid assemblage change in the Burgäschisee core.

Within Zone Burg 1 (1032–951 cm) the assemblages were dominated by *Sergentia coracina*-type with *Paratanytarsus austriacus*-type, *Microtendipes pedellus*-type, *Tanytarsus lugens*-type, *Micropsectra radialis*-type and *Procladius* as subdominant taxa (Fig. 3). In zone Burg 2 (951–844.5 cm) a gradual turnover in chironomid assemblages is observed, with types previously absent beginning to occur and the gradual disappearance of types which were dominant in Burg 1 associated with a moderate increase in chironomid concentrations (Fig. 3). While *Sergentia coracina*-type continued to dominate the assemblage, shifts in the sub-dominant taxa such as *Paratanytarsus austriacus*-type, *Tanytarsus lugens*-type, *Micropsectra radialis*-type, *Protanypus* and *Procladius* occurred. These taxa started to decrease at the onset of Zone Burg 2, coinciding with the first occurrence of *Corynocera oliveri*-type and *Tanytarsus mendax*-type in the record. Later on within Burg 2 other types such as *Chironomus plumosus*-type, *Tanytarus glabrescens*-type, *Tanytarsus lactescens*-type and *Pagastiella* occurred. Zone Burg 3 (844.5–8262 cm) is apparently defined not by the presence of new types, but largely by the disappearance of types present in Zones Burg 1 and Burg 2, such as *Paratanytarsus austriacus*-type and *Protanypus.* Other types which were already present in Burg 2 increased in abundance. The only new type of note is *Polypedilum nubeculosum*-type which appears immediately after the onset of Burg 3. The change in chironomid assemblage into Burg 3 is accompanied by the appearance and abundance changes of many other aquatic invertebrates in the record including large increases in Ceratopogonidae, Ephemeroptera and aquatic/semi terrestrial mites as well as a distinct decline in *Daphnia pulex*-type ephippia.

3.2. Ordination

Axis 1 of a DCA of chironomid assemblages in Burgäschisee explains 31.8% of the variance in the assemblage data and displays little to no change within Burg 1 (Fig. 4). At the onset of Burg 2, DCA axis 1 scores begin to gradually shift to lower values and continue to do so throughout the rest of the zone, representing the gradual change in assemblage composition identified in Fig. 3. Burg 3 represents the lowest DCA axis 1 scores, the culmination of an accelerated change in DCA axis 1 values beginning prior to the end of Burg 2, with the largest DCA axis 1 change recorded at the Burg 2/Burg 3 transition. Together, these results suggest little assemblage change in the oldest sections of the record, the beginning of a gradual trend to assemblages typical for the youngest sections around 940–950 cm and then a more rapid shift to the assemblages dominating in the youngest section at about the Burg 2/Burg transition.

When the Burgäschisee fossil chironomid assemblages are added passively into a DCCA of modern chironomid assemblage data, with axis 1 constrained to represent changes in TP between the modern sites, samples from Burg 1 are characterized by DCCA

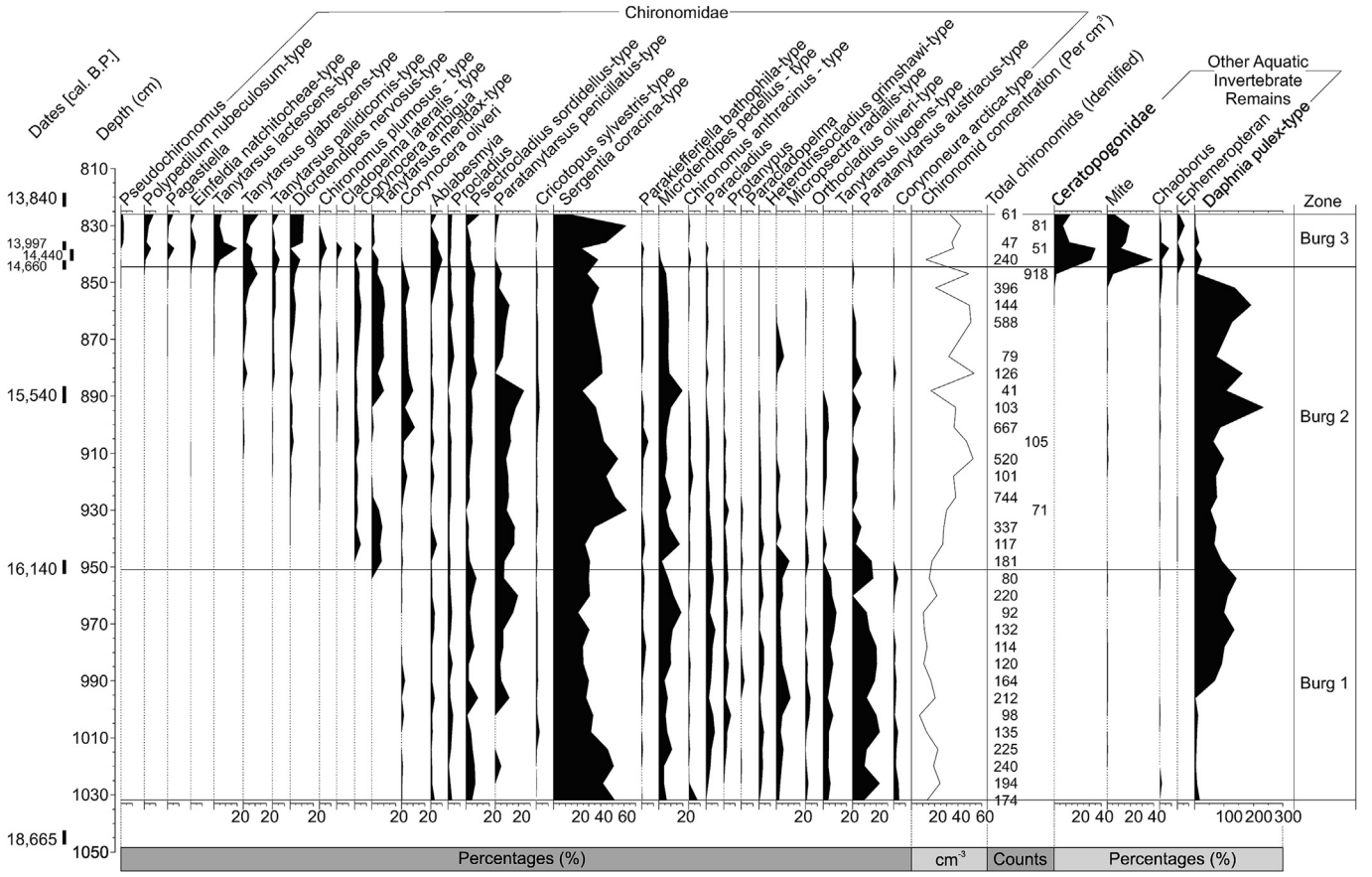

Fig. 3. Fossil chironomid assemblages in the sediments of Burgäschisee. Of the 56 types identified 31 types are shown to document general trends in assemblage turnover. Abundances of chironomid types are shown as a percentage relative to the total number of identified chironomid head capsules whereas other aquatic invertebrate remains are presented as a percentage of the total number of chironomids in a sample including those that were not identified. Ages indicate medians of calibrated age estimates as indicated in Table 1.

axis 1 scores typical for relatively nutrient-poor lakes. DCCA axis 1 scores shift to slightly lower values between ca. 1000 to 900 cm, suggesting that the lake may have experienced a moderate nutrient enrichment in this phase. However, from 900 cm onwards no further shift in DCCA axis 1 scores is apparent, even though major changes in chironomid assemblage composition were registered at Burgäschisee (Figs. 3 and 4).

3.3. Chironomid inferred temperature

Chironomid-inferred mean July air temperatures within Burg 1 show little change and remain ca. 9 °C for most of the zone with some increased variation toward the transition to Burg 2 (Fig. 4). Around the Burg 1/Burg 2 transition, however, inferred temperatures increase to ca. 10 °C and continue to rise gradually to values around 12 °C across zone Burg 2. In contrast, the transition from Burg 2 to Burg 3 is categorised by a rapid increase in temperature from ca. 12 °C–14.5 °C within a relatively short period. In Burg 3 values initially continue to increase, but reach a plateau around ca. 15 °C in the younger part of the zone.

3.4. Reconstruction analogue and performance statistics

Goodness-of-fit statistics indicated that none of the samples in the record have either a “poor fit” or “very poor fit” with temperature (Fig. 4). Analogue statistics showed that only 8 of the samples had no good analogue in the calibration data, whereas most samples (78%) had no close analogue (Fig. 4). *Psectrocladius calcaratus*-type and *Symposiocladius* were the only taxa in the fossil record that were not included in the modern calibration dataset and transfer function. The maximum abundance of these taxa in any sample was 2.0%. Additionally, taxa considered rare (Hill’s N2 < 5) in the training set (*Einfeldia*, *Propsilocerus* and *Paracricotopus*) were present at less than 3% maximum relative abundances in the Burgäschisee record (Fig. 4). Overall the analogue and performance statistics therefore indicate that most taxa in the Burgäschisee record were well represented in the applied transfer function and that, even though close analogues were rare, most fossil samples had a good analogue in the calibration dataset.

4. Discussion

4.1. Chironomid assemblage and lake development

Chironomid assemblages in the early Lateglacial sediments of Burgäschisee are dominated by taxa typically found in cold, oligotrophic lakes in arctic to subarctic environments. For example, *Sergentia coracina*-type, *Micropsectra radialis*-type and *Paratanytarsus austriacus*-type are commonly found in oligotrophic alpine and/or arctic lakes (Brooks and Birks, 2001; Heiri and Lotter, 2010; Heiri et al., 2011). *Sergentia coracina*-type dominates over much of the Burgäschisee sequence. The taxon is eurybathic and typical for lakes that are situated in cold to temperate climates (Brooks et al., 2007; Heiri et al., 2011) and represents oligo-to

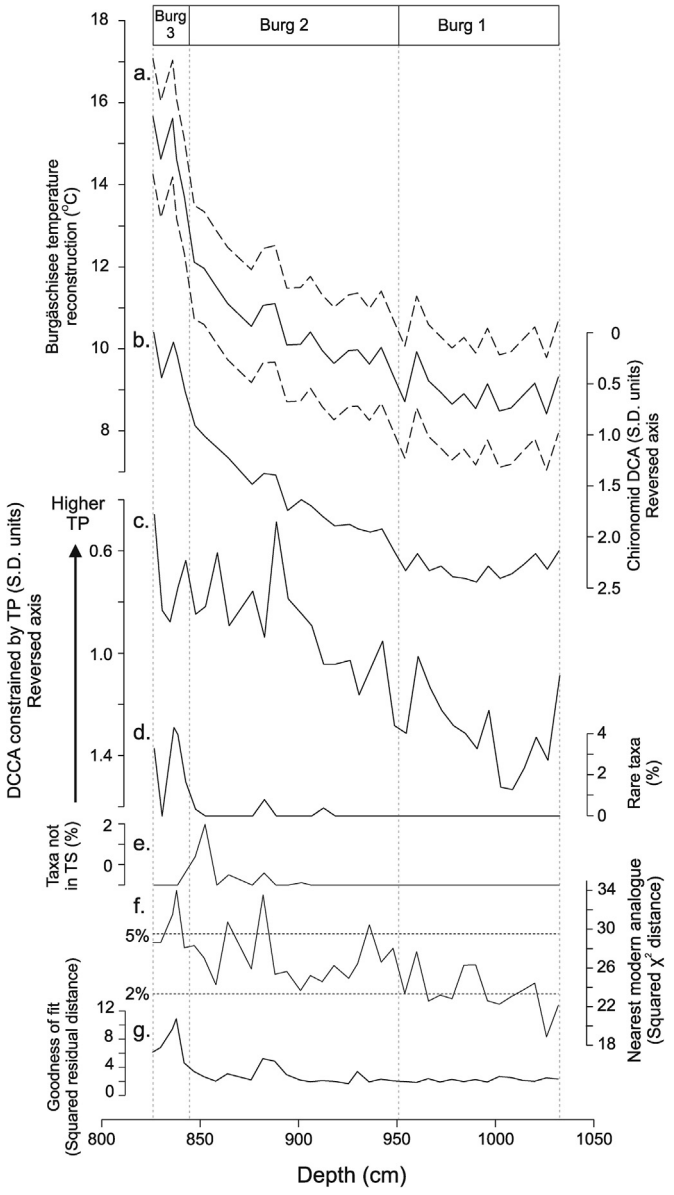

Fig. 4. Chironomid-inferred temperatures from the Burgäschisee record together with ordination results and reconstruction diagnostic statistics. (a) Chironomid-inferred July air temperatures (black solid line) including the sample-specific error of prediction (eSEP; dashed black lines); (b) first axis scores of a DCA of chironomid assemblages in the Burgäschisee record (c) DCCA axis 1 scores for Burgäschisee chironomid samples in DCCA constrained by TP (Verbruggen et al., 2011); see text for details. In this analysis lakes with high TP are characterized by low DCCA axis 1 values as indicated by the arrow; (d) abundance of rare taxa in the Burgäschisee record (N2<5 in the calibration dataset); (e) percentage of taxa in the Burgäschisee record not in the calibration dataset; (f) squared chi-square distance of fossil samples to the nearest modern analogue in the calibration dataset. The horizontal lines indicate thresholds for samples with no close (2%) and no good (5%) analogue in the modern calibration data (following Toth et al., 2015) and (g) goodness of fit statistics. All goodness-of-fit values are well below the thresholds for "poor fit" and "very poor fit" (16.0 and 21.9 respectively) and these threshold values are therefore not indicated.

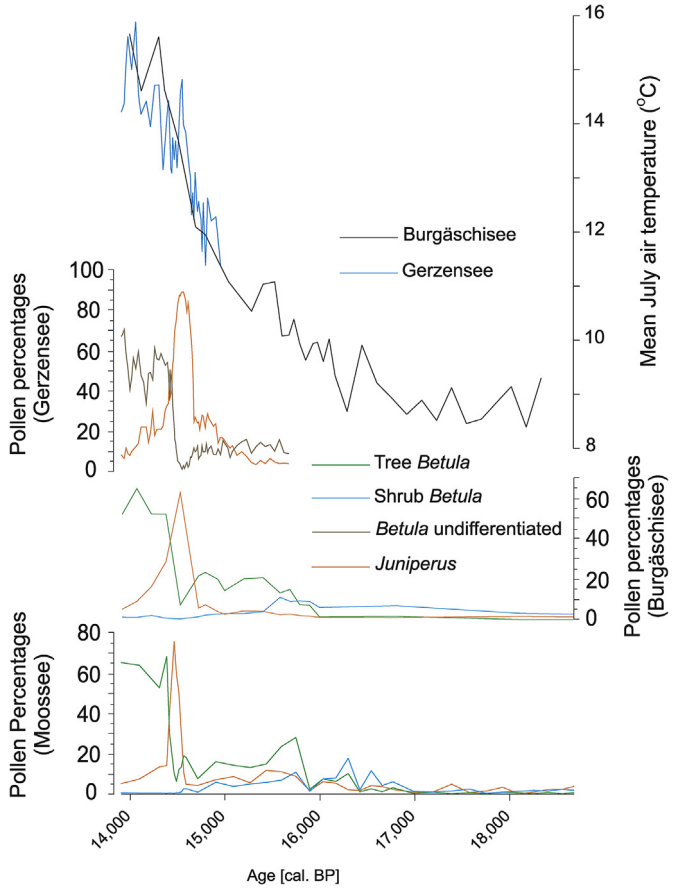

Fig. 5. Chironomid temperature reconstructions from the Northern Swiss Plateau corrected to 465 m a.s.l. (Burgäschisee, this publication; Gerzensee, Lotter et al., 2012) compared with selected pollen types in the Burgäschisee (Rey et al., 2017), Gerzensee (Ammann et al., 2013; shrub *Betula nana* was not separated from tree *Betula* pollen in this study) and Moossee (Rey et al., 2020) records. The Gerzensee record is presented on the age scale of van Raden et al. (2013). For the oldest section we only present samples within 300 years of the Oldest Dryas - Bølling transition, however, since this represents the lowest distinctive age tie point in the Gerzensee record, and lower sections are only very poorly constrained by the available chronological information.

mesotrophic conditions (Brundin, 1956 in Hofmann, 2001). From ca. 16,200 cal. BP (ca. 950 cm) onwards there is a gradual change in chironomid assemblages with taxa typical for warmer climate conditions starting to occur and increasing in abundance, while some taxa that originally dominated in the sequence, such as *Paratanytarsus austriacus*-type and *Micropsectra radialis*-type disappear. For example, the new immigrants *Tanytarsus pallidicornis*-type and *Tanytarsus glabrescens*-type are presently found in subalpine to lowland lakes in the Alps (e.g. Heiri and Lotter, 2010; Heiri et al., 2011). At ca. 14,600 cal. BP (ca. 845 cm), a number of taxa increase which are usually abundant in lowland lakes and temperate climatic conditions, such as *Tanytarsus lactescens*-type and *Polypedilum nubeculosum*-type. At the same time, the abundances of Ceratopogonidae, oribatid mite and chaoborid remains increase. Ceratopogonidae and oribatid mites are common in littoral environments in lakes (e.g. Szadziewski et al., 1997; Solhøy and Solhøy, 2000), particularly in aquatic macrophyte belts, suggesting that the shoreline vegetation may have become more strongly developed and structured in the lake. Chaoborid larvae are common in lakes with seasonal anoxia (Quinlan and Smol, 2010; Ursenbacher et al., 2020). The increase in chaoborids, though not very pronounced, may therefore indicate more stable thermal stratification of the lake and more pronounced anoxia in its deep-water environment.

Overall, the development of chironomid assemblages at Burgäschisee is typical for periods of increasing temperatures, with cold-adapted and oligotrophic taxa dominating the earliest sections of the record and taxa usually found in warmer, more nutrient-rich and oxygen-depleted environments more abundant during the Bølling period (from ca. 14,660 cal. BP/845 cm onwards). The

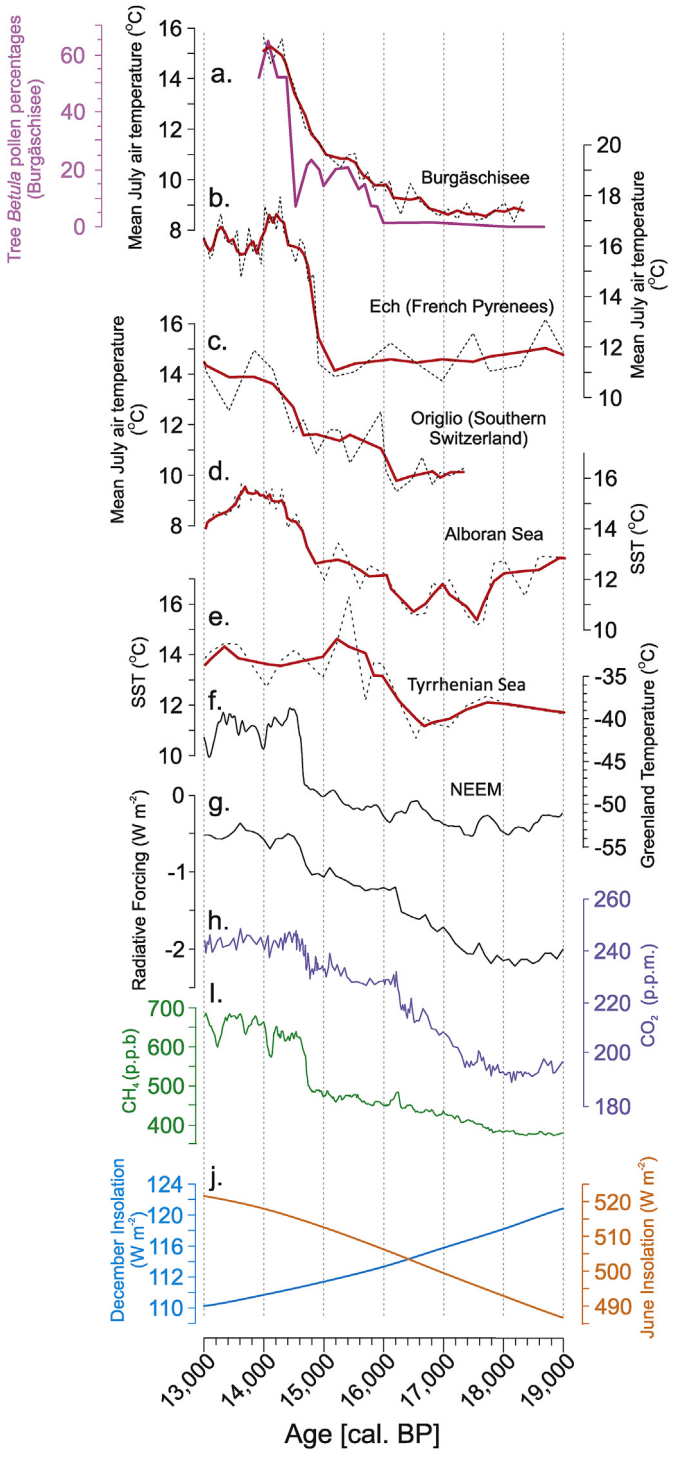

Fig. 6. Palaeotemperature records for the early Late Glacial. For temperature records (plots a. - e.) the dashed black line represents unsmoothed values whereas the solid red line represents a three sample running average. a. Burgäschisee chironomid temperature record from the Swiss lowlands and Burgäschisee tree *Betula* pollen percentages (solid pink line, Rey et al., 2017); b. Ech Palaeolake chironomid-inferred temperature (Data digitized from Millet et al., 2012); c. Lago di Origlio chironomid-inferred temperature (Samartin et al., 2012); d. Alboran sea surface temperature (SST; Cacho et al., 2001); e. Tyrrhenian SST (Cacho et al., 2001); f. NEEM temperature reconstruction (Buizert et al., 2014); g. Total radiative forcing from greenhouse gasses (Schilt et al., 2010; Marcott et al., 2014); h. CO_2 from West Antarctic Ice Sheet Divide ice core (WDC; Marcott et al., 2014); i: CH_4 from WDC (WAIS Divide Project Members, 2013; Marcott et al., 2014) and j. Summer and December insolation curves for 45°N (Berger and Loutre, 1991). (For interpretation of the references to colour in this figure legend, the reader is referred to the Web version of this article.)

strongest shift in assemblage composition occurred at the transition between chironomid zones Burg 2 and 3, which coincides with the Oldest Dryas/Bølling transition, as is clearly indicated by both changes in DCA axis 1 scores (Fig. 4) and the statistically significant zonal boundary identified at this transition by CONISS (Fig. 3). However, the trend in assemblage composition clearly started much earlier with the onset of Burg 2, at ca. 16,200 cal. BP (ca. 950 cm). Temperatures tend to co-vary with nutrient availability, and in consequence often also oxygen availability for deepwater fauna in lakes. This can be observed among modern lakes, e.g. as represented in chironomid-temperature calibration datasets (Brodersen and Anderson, 2002; Heiri and Lotter, 2005). However, similar patterns are apparent in downcore records as well where assemblages of cold-indicating chironomids also tend to be dominated by taxa adapted for oxygen-rich and nutrient-poor conditions (e.g. Hofmann, 2001; Velle et al., 2010), whereas warm-adapted assemblages are often dominated by more eutrophic taxa that are also better able to survive low oxygen conditions (Brodersen and Anderson, 2002; Eggermont and Heiri, 2012). To explore the extent to which chironomid assemblage change in the Burgäschisee record can be explained by changes in nutrient concentrations, rather than temperatures, we compared downcore trajectories in chironomid assemblage composition with modern (subfossil) chironomid assemblages in 28 deep lakes across Europe (Verbruggen et al., 2011) using direct gradient analysis (Fig. 4). Since these lakes are all deep and stratified (max. water depth mostly 30 m and deeper), it can be expected that between-lake variations in chironomid assemblage composition in this dataset are mainly driven by nutrient and oxygen concentrations rather than air or surface water temperatures (Verbruggen et al., 2011). The results of this analysis revealed that there is some co-variation in chironomid assemblage changes toward assemblage states typical for more nutrient-rich lakes (indicated by DCCA axis 1 values, Fig. 4c) and towards assemblages typical for warmer lakes (indicated by chironomid-inferred temperatures, Fig. 4b). However, the trend toward assemblages representative for nutrient-rich, stratified lakes appears to start well before the trend towards assemblages typical for warmer lakes (Fig. 4). Furthermore, after 15,600 cal BP (ca. 894 cm), when chironomid-inferred temperatures were clearly increasing, there is no evidence for shifts in the DCCA towards assemblage states typical for more nutrient-rich lakes. These analyses therefore suggest that, even though there will have been some co-variation between increasing temperatures and increasing nutrient concentrations at Burgäschisee during the Lateglacial, as can be expected based on other Lateglacial chironomid records from Europe (e.g. Brooks and Birks, 2001; Heiri and Millet, 2005), shifts towards assemblages typical for warmer lake ecosystems cannot be easily explained simply by the increasing nutrient concentrations in the lake. Instead, these shifts, particularly from 15,600 cal. BP onwards, seem to be mainly driven by increasing temperature, without a corresponding trajectory towards assemblage composition typical for more nutrient-rich lakes.

S. coracina-type, which dominates throughout the Burgäschisee record, is able to survive in cool arctic to subarctic lakes, but also in temperate lakes where thermal stratification maintains a cool profundal zone (Hofmann, 2001) as long as that the trophic state is oligo-mesotrophic and allows sufficient oxygen below the thermocline (Brundin, 1956 in Hofman, 2001). Based on the modern water depth, and the length of the sediment sequence, Burgäschisee may have been as deep as 39–41 m during the early late glacial. Hypolimnetic oxygen apparently remained high enough to allow the survival of *S. coracina*-type in the deep, cold profundal habitats of the lake even in the temperate climate conditions after the Oldest Dryas – Bølling transition. It could be expected that the persistence of a large, cool profundal compartment, and of those

chironomid types inhabiting it, could influence the temperature reconstruction, leading to a depression in reconstructed temperatures and a more gradual transition of chironomid assemblages than expected for shallower lakes. However, in our record the transition between Burg 2 and 3 coincided perfectly with the transition between the Oldest Dryas and Bølling zones and local reforestation as represented in the Burgäschisee pollen record (Rey et al., 2017), speaking against such a delayed response of chironomid assemblages in the lake. Furthermore, absolute values of the Burgäschisee chironomid-inferred temperature reconstruction agree well with a similar reconstruction from a shallow water (littoral) sediment core from Lake Gerzensee (see 4.2.2, below), suggesting that the depth of the lake did not lead to a significant depression of chironomid-based temperature inferences at Burgäschisee.

4.1.1. Comparison of the new temperature record with regional vegetation development

The Burgäschisee chironomid record has provided the first well dated high-resolution Early Lateglacial temperature reconstruction in the Northern Swiss lowlands that is not based on vegetation proxies. It covers almost the entire period, from landscape stabilisation after glacial termination and retreat, to the Bølling interstadial. Chironomid remains were abundant enough for inferring temperatures immediately after sands are no longer deposited into the lake (ca. 18,300 cal. B.P.). Between ca. 18,300–16,100 cal. BP the temperature reconstruction indicates relatively stable low July air temperatures of ca. 9 °C (Fig. 5), values 9–10 °C cooler than today. This is in agreement with the Burgäschisee pollen record which indicates a tree-less steppe tundra dominated by a diverse array of herb flora as well as thickets of small shrubs, including the dwarf birch *Betula nana* (Rey et al., 2017). Furthermore, this finding agrees with other pollen records from lowland Switzerland which consistently indicate a tundra environment for this time period (e.g. Rey et al., 2020; Beckmann et al., 2004; Lotter et al., 1999; Lotter and Zbinden, 1989). At present, the potential upper, temperature-limited treeline in the Alps coincides with mean July air temperatures around 7.5–9.5 °C (Landolt, 2003), and therefore inferred July air temperatures are consistent with the palaeovegetation data.

At ca. 16,200 cal. BP (broadly correlating with the transition to chironomid assemblage zone Burg 2) chironomid-inferred July air temperatures at Burgäschisee increase from ca. 9 °C to ca. 10 °C (Fig. 5). This increase corresponds with the increase in shrub pollen in the Burgäschisee record, particularly of *Betula nana, Salix,* and *Juniperus*. Furthermore *Betula* trees expanded, likely forming first stands in the tundra (Rey et al., 2017, Fig. 5), even though the vegetation around Burgäschisee remained dominated by herbs. This implies a transition from a herb-dominated steppe tundra to shrub tundra, with tree stands or small woodlands dominated by *Betula* occupying favourable sites. Palaeobotanical data from other pollen records across the northern Swiss lowlands display a similar vegetational reorganisation at other sites (e.g. Lotter, 1999; Beckmann et al., 2004; Rey et al., 2020) prior to afforestation at 14,700 cal. BP. It has been suggested that the early expansion of shrub tundra may have been the consequence of delayed pedogenesis and associated increase in nutrient availability for terrestrial plants (Ammann et al., 1983). However, glaciological evidence suggests that glacier retreat occurred as early as ca. 19,000 cal. BP (±1000 years) (Ivy Ochs et al., 2004) in the study region which is in excellent agreement with the oldest radiocarbon dated lake sediment sequences on the Swiss Plateau which reach back to as early as 19,180 cal. BP at Moossee (Rey et al., 2020). This would imply a 3000-year period in which pedogenesis did not modulate vegetational distributions, followed by a near synchronous vegetational composition shift across the entire northern Swiss lowlands. As Rey et al. (2017; 2020) point out, it seems more likely that after initial pedogenesis and landscape stabilisation a synchronous and regional increase in July temperature above 10 °C enabled shrub and tree taxa to establish and expand in lowland Switzerland. Our new temperature record from Burgäschisee indicates a clear shift towards chironomid assemblages typical for higher temperatures at this transition, and, as consequence an increase in chironomid-inferred temperatures that coincides with this vegetation change. This provides clear support for the hypothesis that an increase in summer temperatures is responsible for this observed, large-scale vegetation change on the Swiss Plateau before afforestation at 14,700 cal. BP.

Chironomid-inferred temperatures in the Burgäschisee record continue to increase throughout zone Burg 2, reaching values as high as 12–12.5 °C while the vegetation composition established after the temperature increase at ca. 16,000 cal. BP does not change significantly. The temperature rise culminates in a rapid temperature increase from ca. 12.0–15 °C at the transition from Burg 2 into Burg 3 (Fig. 5), coinciding with the Oldest Dryas/Bølling transition in the pollen record. In other pollen profiles and palaeotemperature reconstructions from Switzerland the temperature increase associated with the Oldest Dryas/Bølling transition has been estimated to have taken place very rapidly with a duration between 40 and 95 years (van Raden et al., 2013; Luetscher et al., 2015). At Burgäschisee, this transition seems to occur slightly more slowly, but this may be the consequence of a relatively low sampling resolution in the chironomid record during this transition as well as of the dating uncertainty. This transition occurs synchronously with reorganisations of vegetation around Burgäschisee with an initial short-lived increase in *Juniperus* pollen (up to 60%; Fig. 5), typical for Lateglacial afforestation in lowland Switzerland, followed by an increase in *Betula* pollen representative for tree *Betula* species in the pollen record (Rey et al., 2017). This finding agrees well with other climate records from Central Europe which consistently indicate a rapid warming phase at the Oldest Dryas/Bølling transition. For example, oxygen isotope records from speleothem and lake marl sequences indicate a rapid increase in temperature at ca. 14,700 cal. B.P. (Lotter et al., 1992, 2012; van Raden et al., 2013; Luetscher et al., 2015).

4.1.2. Burgäschisee chironomid-inferred temperatures compared with other climate reconstructions

The Burgäschisee record represents one of the few, well-dated palaeoclimate records from Southwestern Central Europe with independent age estimates older than the Oldest Dryas/Bølling transition. In the lowest section between ca. 18,300–16,200 cal. BP, July air temperatures of ca. 9 °C are inferred. These temperatures agree with the vegetation reconstructions for lowland Switzerland at this time interval, which indicate a treeless tundra environment with some shrub elements (see section 4.2.1.). Furthermore, similar July air temperature values 8–10 °C below modern have also been reported for full glacial conditions based on climate model-based estimates for the study region (e.g. Ludwig et al., 2017). During the start of the first warming phase at ca. 16,200–16,000 cal. BP, chironomid-inferred temperatures increase to around 10 °C. This again agrees with the vegetation reconstruction which indicates a change from a largely treeless environment to a tree-shrub tundra at this time, a vegetation transition which at the alpine treeline can presently be observed at July air temperatures around 7.5–9.5 °C (Landolt, 2003). From the latest sections of the Oldest Dryas onwards several other quantitative temperature records are available from Central Europe (Heiri et al., 2014). The second available chironomid-based July air temperature reconstruction from the Swiss Plateau originates from Gerzensee, 58 km from Burgäschisee.

This lake sediment record extends ca. 40 cm below the Oldest Dryas/Bølling transition (Lotter et al., 2012; Brooks and Heiri, 2013). However, since there is no reliable basal age constraint for this sequence it remains unclear how rapid sedimentation rates are in this section of the record which essentially remains undated. In the sediments just preceding the Oldest Dryas/Bølling transition chironomid-inferred temperatures of 12 °C are recorded, values very similar to the reconstructed temperatures at Burgäschisee of ca. 11.5 °C (Fig. 5). At the transition, both the Burgäschisee and Gerzensee chironomid records indicate a rapid increase of July air temperatures from ca. 12 to ca. 15 °C, followed by a more gradual increase during the early Bølling period.

The increase in temperature at the Oldest Dryas/Bølling transition in the Burgäschisee and Gerzensee records is of similar amplitude as the increase by 2–3 °C inferred for this transition in the French Jura mountains (Heiri and Millet, 2005) and Central Switzerland (Larocque et al., 2010) based on chironomids, and for the Swiss Plateau based on mixed aquatic insect taxa (Elias and Wilkinson, 1983). Additionally, both the Burgäschisee record and that of Heiri and Millet (2005) display a gradual temperature increase in the early Bølling which is in agreement with the increasing summer insolation values during the Lateglacial interstadial (Berger and Loutre, 1991), and, e.g., the oxygen isotope-based reconstructions of mean annual air temperature from Ammersee and Gerzensee (von Grafenstein et al., 1999, 2013). In contrast, some other summer temperature reconstructions from Northern Switzerland, for example pollen-based reconstructions (e.g. Lotter et al., 2012) show a more pronounced warming at the Oldest Dryas/Bølling transition and higher early Bølling than late Bølling temperatures. Lotter et al. (2012) discuss that this discrepancy may be due to temperatures during different seasons than summer and/or precipitation influencing vegetation in the Swiss Plateau during this interval.

The temperature development inferred by chironomids at Burgäschisee is also consistent with the inferred glacier retreat after the end of the Last Glacial Maximum in Northern Switzerland. Several phases of glacier retreat suggest warming episodes well before the Oldest Dryas/Bølling transition, including at ca. 16,000 cal. BP (e.g. Ivy-Ochs et al., 2008; Heiri et al., 2014). However, further phases of glacier retreats between 18,000 and 14,700 cal. BP are inferred based on past glacier extent, which are not represented as warming phases in our chironomid record (Ivy-Ochs et al., 2008). This may be because glaciation and glacier extent are not only determined by summer temperatures but also precipitation, local humidity and other factors that influence glacier extent and ice dynamics (Kerschner and Ivy-Ochs, 2008).

Additional chironomid-based reconstructions that encompass the period 16,000–14,700 cal. BP and are reliably dated in this interval are available from south of the Alps, from the Ticino region of Southern Switzerland (Lago di Origlio, Samartin et al., 2012), and from Western France in the Northern Pyrenees (Ech Palaeolake; Millet et al., 2012). These reconstructions agree with the Burgäschisee record in that a distinct increase in July air temperatures is inferred at the Oldest Dryas/Bølling transition, i.e. an abrupt temperature increase in the range of 2–5 °C (Fig. 6). However, as discussed in Samartin et al. (2012) temperatures in the Lago di Origlio record show a stepwise increase for the pre-Bølling, with a distinct increase by ca. 2.5 °C recorded at ca. 16,000 cal. BP followed by a relatively stable period prior to the temperature rise at the transition to the Bølling. This pre-Bølling increase at 16,000 cal. BP coincides with reforestation in Northern Italy and other sections of the northern Mediterranean region (Samartin et al., 2012), with increases in sea-surface temperatures inferred from marine records in the Mediterranean (Cacho et al., 2001), as well as with climatic ameliorations inferred from speleothems for the Eastern Mediterranean region (e.g. Fleitmann et al., 2009). In contrast, the chironomid-inferred record from the Ech palaeolake, situated in the northern Pyrenees only 128 km from the Atlantic coastline, displays no clear trend in temperatures during the pre-Bølling period. It seems therefore that changes in chironomid-inferred temperatures at Burgäschisee can be interpreted as intermediate between the situation at Ech, which during the entire period ca. 19,000 to 14,700 cal. BP was apparently influenced by the prevailing cold conditions over the North Atlantic resulting in the maintenance of low temperatures (Millet et al., 2012; Martínez-García et al., 2015); and Lago di Origlio where the chironomid-based temperature reconstruction displays a stepwise increase with a distinct pre-Bølling warming occurring at 16,000 cal. BP. Lago di Origlio has a climate typical for the Southern Alps, shielded from both Northern and Western air masses by the Alpine arc and presently maintaining an “Insubrian” climate (Brzeziecki et al., 1995) in which temperatures are close to those of more southern regions of the Mediterranean area (Bugmann, 1996). Therefore, it is not surprising that the temperature reconstruction from this site shows a similar temperature development as seen in records from the Mediterranean Sea (Alboran and Tyrrhenian seas; Cacho et al., 2001), which also show a clear increase in temperature from ca. 16,200 cal. BP onwards (Fig. 6). Presently the climate in the region of Burgäschisee is characterized by a strong westerly influence (National Centre for Climate Services, 2014), both during the winter and summer months. Although significant air circulation pattern changes have been suggested for the last deglaciation (e.g. Luetscher et al., 2015; Becker et al., 2016), it can be expected that a significant westerly influence will have prevailed during the entire Lateglacial period. At the same time increasing summer insolation and greenhouse gas concentrations would have promoted increasing summer temperatures, explaining the “mixed” pattern of temperature changes at Burgäschisee intermediate between the situation at Ech and Lago di Origlio.

5. Conclusions

Our new, quantitative summer temperature reconstruction from northern Switzerland, together with recent palynological results demonstrating distinct vegetation changes on the Swiss Plateau around ca. 16,000 (Rey et al., 2017; 2020), indicate that summer temperatures were increasing in this region well before the major Lateglacial warming inferred at the Oldest Dryas/Bølling transition at ca. 14,700 cal. BP. This pattern agrees with temperature variations reported for lower latitude regions of Europe (e.g. Fletcher et al., 2010). It is also consistent with the increasing greenhouse gas concentrations and Northern hemisphere summer insolation values, as these would be expected to lead to progressively warmer summer climate in large sections of the northern hemisphere during this time interval. Our results therefore suggest that even though large parts of Central and Northern Europe were still covered by tundra to steppe vegetation during the period ca. 19,000 to 14,700 cal. BP (Rey et al., 2017; 2020), distinct warming trends may already have influenced summer temperatures at least in the southwestern sector of Central Europe. They also challenge the conventional view that major parts of Central and Northwestern Europe did not show major Lateglacial warming prior to 14,700 cal. BP, an interpretation that is in agreement with $\delta^{18}O$ records from the GRIP and GISP ice core records from Greenland (Johnsen et al., 2001), which also do not show major warming prior to this date. In this context it is interesting to note that temperature reconstructions from the Greenland ice cores which take into account additional information next to the $\delta^{18}O$ record, such as combined reconstructions based on borehole temperature and $\delta^{18}O$ (GRIP ice core, Johnsen et al., 2001) or $\delta^{15}N\text{-}N_2$ (Neem ice core,

Buizert et al., 2014) show evidence for a similar early Lateglacial warming as recorded in our new Burgäschsee record (Fig. 6). This suggests that also Greenland and possibly other parts of the northern circum-Atlantic region may have been affected by such an early pre-Bøllling Lateglacial warming.

Author statement

Alexander Bolland and Oliver Heiri: Conceptualization, Methodology, Validation, Formal Analysis, Writing - Original Draft and Project administration. Alexander Bolland, Erika Gobet, Fabian Rey: Investigation. Alexander Bolland: Data curation and Visualization. Oliver Heiri, Fabian Rey, Erika Gobet, Willy Tinner: Supervision. Oliver Heiri: Funding acquisition. Alexander Bolland, Oliver Heiri, Erika Gobet, Willy Tinner and Fabian Rey: Resources and Writing - Review & Editing.

Data availability

Chironomid data associated with this study as well as the chironomid-inferred temperature data have been deposited at the Dryad online data repository: https://doi.org/10.5061/dryad.08kprr509 (www.datadryad.org/).

Declaration of competing interest

The authors declare that they have no known competing financial interests or personal relationships that could have appeared to influence the work reported in this paper.

Acknowledgments

We thank all members of the field work team: Willi Tanner, Richard Niederreiter, André F. Lotter, Claire Rambeau, Marianne Steffen, Camilla Calò, Stéphanie Samartin, Elisa Vescovi, Stefanie Wirth, Stewart Bishop, Martin Tschanz and Florencia Oberli. We also thank both reviewers for helpful suggestions that have improved our manuscript. This research has been supported by the Swiss National Science Foundation (SNSF grant 200021_165494).

Appendix A. Supplementary data

Supplementary data to this article can be found online at https://doi.org/10.1016/j.quascirev.2020.106484.

References

Allen, J.R., Watts, W.A., Huntley, B., 2000. Weichselian palynostratigraphy, palaeovegetation and palaeoenvironment; the record from Lago Grande di Monticchio, southern Italy. Quat. Int. 73, 91–110.
Ambühl, H., Stumm, W., 1984. Bericht über die Auswirkungen der Tiefenwasserableitung im Burgäschisee. EAWAG.
Ammann, B., Chaix, L., Eicher, U., Elias, S.A., Gaillard, M.J., Hofmann, W., Siegenthaler, U., Tobolski, K., Wilkinson, B., 1983. Vegetation, insects, molluscs and stable isotopes from late Würm deposits at Lobsigensee (Swiss Plateau). Studies in the late Quaternary of Lobsigensee 7. Rev. Paleobiol. 2, 221–227.
Ammann, B., van Leeuwen, J.F., van der Knaap, W.O., Lischke, H., Heiri, O., Tinner, W., 2013. Vegetation responses to rapid warming and to minor climatic fluctuations during the Late-Glacial Interstadial (GI-1) at Gerzensee (Switzerland). Palaeogeogr. Palaeoclimatol. Palaeoecol. 391, 40–59.
Andersen, T., Cranston, P.S., Epler, J.H. (Eds.), 2013. Chironomidae of the Holarctic Region: Keys and Diagnoses: Larvae. Scandinavian Society of Entomology.
Arn, H., 1945. Die Melioration des Gebietes um den Burgäschisee und die See-Absenkung. Verlag nicht ermittelbar.
Becker, P., Seguinot, J., Jouvet, G., Funk, M., 2016. Last Glacial Maximum precipitation pattern in the Alps inferred from glacier modelling. Geograph. Helv. 71 (3), 173–187.
Beckmann, M., 2004. Pollenanalytische Untersuchung der Zeit der Jäger und Sammler und der ersten Bauern an zwei Lokalitäten des Zentralen Schweizer Mittellandes. Diss. Bot. 390, 1–223.
Bennett, K.D., 1996. Determination of the number of zones in a biostratigraphical sequence. New Phytol. 132 (1), 155–170.
Berger, A., Loutre, M.F., 1991. Insolation values for the climate of the last 10 million years. Quat. Sci. Rev. 10 (4), 297–317.
Birks, H.J.B., Braak, C.T., Line, J.M., Juggins, S., Stevenson, A.C., 1990. Diatoms and pH reconstruction. Philos. Trans. Roy. Soc. B 327 (1240), 263–278.
Birks, H.J.B., Heiri, O., Seppä, H., Bjune, A.E., 2010. Strengths and weaknesses of quantitative climate reconstructions based on Late-Quaternary. Open Ecol. J. 3 (1), 68–110.
Birks, H.H., Aarnes, I., Bjune, A.E., Brooks, S.J., Bakke, J., Kühl, N., Birks, H.J.B., 2014. Lateglacial and early-Holocene climate variability reconstructed from multi-proxy records on Andøya, northern Norway. Quat. Sci. Rev. 89, 108–122.
Blaauw, M., 2010. Methods and code for 'classical'age-modelling of radiocarbon sequences. Quat. Geochronol. 5 (5), 512–518.
Bugmann, H.K., 1996. A simplified forest model to study species composition along climate gradients. Ecology 77 (7), 2055–2074.
ter Braak, C.J., Juggins, S., 1993. Weighted averaging partial least squares regression (WA-PLS): an improved method for reconstructing environmental variables from species assemblages. In: Twelfth International Diatom Symposium. Springer, Dordrecht, pp. 485–502.
ter Braak, C.J.F., Juggins, S., Birks, H.J.B., Van der Voet, H., 1993. Weighted averaging partial least squares regression (WA-PLS): definition and comparison with other methods for species-environment calibration. In: Multivariate Environmental Statistics, vol. 6. Elsevier, pp. 525–560.
ter Braak, J.F., Smilauer, P., 2018. Canoco Reference Manuel and User's Guide: Software for Ordination (Version 5.10). Microcomputer Power, Ithaca, NY, USA), p. 536.
Brodersen, K.P., Anderson, N.J., 2002. Distribution of chironomids (Diptera) in low arctic West Greenland lakes: trophic conditions, temperature and environmental reconstruction. Freshw. Biol. 47 (6), 1137–1157.
Brodersen, K.P., Quinlan, R., 2006. Midges as palaeoindicators of lake productivity, eutrophication and hypolimnetic oxygen. Quat. Sci. Rev. 25 (15–16), 1995–2012.
Brooks, S.J., 2006. Fossil midges (Diptera: Chironomidae) as palaeoclimatic indicators for the Eurasian region. Quat. Sci. Rev. 25 (15–16), 1894–1910.
Brooks, S.J., Birks, H.J.B., 2000. Chironomid-inferred Late-glacial air temperatures at Whitrig Bog, southeast Scotland. J. Quat. Sci. 15 (8), 759–764.
Brooks, S.J., Birks, H.J.B., 2001. Chironomid-inferred air temperatures from Late-glacial and Holocene sites in north-west Europe: progress and problems. Quat. Sci. Rev. 20 (16–17), 1723–1741.
Brooks, S.J., Heiri, O., 2013. Response of chironomid assemblages to environmental change during the early Late-glacial at Gerzensee, Switzerland. Palaeogeogr. Palaeoclimatol. Palaeoecol. 391, 90–98.
Brooks, S.J., Langdon, P.G., Heiri, O., 2007. The Identification and Use of Palaeartic Chironomidae Larvae in Palaeoecology. QRA Technical guide No10. Quaternary Research Association, London UK, p. 276.
Brundin, L., 1956. Die bodenfaunistischen Seetypen und ihre Anwendbarkeit auf die Südhalbkugel. Zugleich eine Theorie der produktionsbiologischen Bedeutung der glazialen Erosion. Inst. Freshw. Res. Drottningholm Rep. 37, 186–235.
Brzeziecki, B., Kienast, F., Wildi, O., 1995. Modelling potential impacts of climate change on the spatial distribution of zonal forest communities in Switzerland. J. Veg. Sci. 6 (2), 257–268.
Buizert, C., Gkinis, V., Severinghaus, J.P., He, F., Lecavalier, B.S., Kindler, P., Leuenberger, M., Carlson, A.E., Vinther, B., Masson-Delmotte, V., White, J.W., 2014. Greenland temperature response to climate forcing during the last deglaciation. Science 345 (6201), 1177–1180.
Cacho, I., Grimalt, J.O., Canals, M., Sbaffi, L., Shackleton, N.J., Schönfeld, J., Zahn, R., 2001. Variability of the western Mediterranean Sea surface temperature during the last 25,000 years and its connection with the Northern Hemisphere climatic changes. Paleoceanography 16 (1), 40–52.
Clark, P.U., Dyke, A.S., Shakun, J.D., Carlson, A.E., Clark, J., Wohlfarth, B., Mitrovica, J.X., Hostetler, S.W., McCabe, A.M., 2009. The last glacial maximum. Science 325 (5941), 710–714.
Clark, P.U., Shakun, J.D., Baker, P.A., Bartlein, P.J., Brewer, S., Brook, E., Carlson, A.E., Cheng, H., Kaufman, D.S., Liu, Z., Marchitto, T.M., 2012. Global climate evolution during the last deglaciation. Proc. Natl. Acad. Sci. Unit. States Am. 109 (19), 1134–1142.
Duprat-Oualid, F., Rius, D., Bégeot, C., Magny, M., Millet, L., Wulf, S., Appelt, O., 2017. Vegetation response to abrupt climate changes in Western Europe from 45 to 14.7 k cal a BP: the Bergsee lacustrine record (Black Forest, Germany). J. Quat. Sci. 32 (7), 1008–1021.
Eggermont, H., Heiri, O., 2012. The chironomid-temperature relationship: expression in nature and palaeoenvironmental implications. Biol. Rev. 87 (2), 430–456.
Eicher, U., Siegenthaler, U., 1976. Palynological and oxygen isotope investigations on Late-Glacial sediment cores from Swiss lakes. Boreas 5 (2), 109–117.
Elias, S.A., Wilkinson, B., 1983. Lateglacial insect fossil assemblages from Lobsigensee (Swiss plateau). Studies in the late quaternary of Lobsigensee 3. Rev. Paleobiol. 2 (2), 189–204.
Fischer, H., Behrens, M., Bock, M., Richter, U., Schmitt, J., Loulergue, L., Chappellaz, J., Spahni, R., Blunier, T., Leuenberger, M., Stocker, T.F., 2008. Changing boreal methane sources and constant biomass burning during the last termination. Nature 452 (7189), 864–867.
Fleitmann, D., Cheng, H., Badertscher, S., Edwards, R.L., Mudelsee, M., Göktürk, O.M., Fankhauser, A., Pickering, R., Raible, C.C., Matter, A., Kramers, J., 2009. Timing

and climatic impact of Greenland interstadials recorded in stalagmites from northern Turkey. Geophys. Res. Lett. 36 (19) https://doi.org/10.1029/2009GL040050.
Fletcher, W.J., Goñi, M.F.S., 2008. Orbital-and sub-orbital-scale climate impacts on vegetation of the western Mediterranean basin over the last 48,000 yr. Quat. Res. 70 (3), 451–464.
Fletcher, W.J., Goñi, M.S., Peyron, O., Dormoy, I., 2010. Abrupt climate changes of the last deglaciation detected in a Western Mediterranean forest record. Clim. Past 6, 245–264.
von Grafenstein, U., Erlenkeuser, H., Brauer, A., Jouzel, J., Johnsen, S.J., 1999. A mid-European decadal isotope-climate record from 15,500 to 5000 years BP. Science 284 (5420), 1654–1657.
von Grafenstein, U., Belmecheri, S., Eicher, U., van Raden, U.J., Erlenkeuser, H., Andersen, N., Ammann, B., 2013. The oxygen and carbon isotopic signatures of biogenic carbonates in Gerzensee, Switzerland, during the rapid warming around 14,685 years BP and the following interstadial. Palaeogeogr. Palaeoclimatol. Palaeoecol. 391, 25–32.
Grimm, E.C., 1987. CONISS: a FORTRAN 77 program for stratigraphically constrained cluster analysis by the method of incremental sum of squares. Comput. Geosci. 13 (1), 13–35. https://doi.org/10.1016/0098-3004(87)90022-7.
Guthruf, J., Zeh, M., Guthruf-Seiler, K., 1999. Kleinseen im Kanton Bern. Amt für Gewässerschutz und Abfallwirtschaft des Kantons Bern. Gewässer-und Bodenschutzlabor, pp. 32–34.
He, F., Shakun, J.D., Clark, P.U., Carlson, A.E., Liu, Z., Otto-Bliesner, B.L., Kutzbach, J.E., 2013. Northern Hemisphere forcing of Southern Hemisphere climate during the last deglaciation. Nature 494 (7435), 81–85.
Heiri, O., Lotter, A.F., 2001. Effect of low count sums on quantitative environmental reconstructions: an example using subfossil chironomids. J. Paleolimnol. 26 (3), 343–350.
Heiri, O., Lotter, A.F., Hausmann, S., Kienast, F., 2003. A chironomid-based Holocene summer air temperature reconstruction from the Swiss Alps. Holocene 13 (4), 477–484.
Heiri, O., Lotter, A.F., 2005. Holocene and Lateglacial summer temperature reconstruction in the Swiss Alps based on fossil assemblages of aquatic organisms: a review. Boreas 34 (4), 506–516.
Heiri, O., Millet, L., 2005. Reconstruction of late glacial summer temperatures from chironomid assemblages in lac Lautrey (Jura, France). J. Quat. Sci. 20 (1), 33–44.
Heiri, O., Cremer, H., Engels, S., Hoek, W.Z., Peeters, W., Lotter, A.F., 2007a. Late-glacial summer temperatures in the Northwest European lowlands: a chironomid record from Hijkermeer, The Netherlands. Quat. Sci. Rev. 26 (19–21), 2420–2437.
Heiri, O., Filippi, M.L., Lotter, A.F., 2007b. Lateglacial summer temperature in the Trentino area (Northern Italy) as reconstructed by fossil chironomid assemblages in Lago di Lavarone (1100 m asl). Studi Trentini Sci. Nat. Acta Geol. 82, 299–308.
Heiri, O., Lotter, A.F., 2010. How does taxonomic resolution affect chironomid-based temperature reconstruction? J. Paleolimnol. 44 (2), 589–601.
Heiri, O., Brooks, S.J., Birks, H.J.B., Lotter, A.F., 2011. A 274-lake calibration data-set and inference model for chironomid-based summer air temperature reconstruction in Europe. Quat. Sci. Rev. 30 (23–24), 3445–3456.
Heiri, O., Koinig, K.A., Spotl, C., Barrett, S., Brauer, A., Drescher-Schneider, R., Gaar, D., Ivy-Ochs, S., Kerschner, H., Luetscher, M., Moran, A., Nicolussi, K., Preusser, F., Schmidt, R., Schoeneich, P., Schworer, C., Sprafke, T., Terhorst, B., Tinner, W., 2014. Palaeoclimate records 60-8 ka in the Austrian and Swiss Alps and their forelands. Quat. Sci. Rev. 106, 186–205. https://doi.org/10.1016/j.quascirev.2014.05.021.
Hughes, A.L., Gyllencreutz, R., Lohne, Ø.S., Mangerud, J., Svendsen, J.I., 2016. The last Eurasian ice sheets–a chronological database and time-slice reconstruction, DATED-1. Boreas 45 (1), 1–45.
Hoek, W.Z., Bohncke, S.J.P., 2002. Climatic and environmental events over the Last Termination, as recorded in The Netherlands: a review. Neth. J. Geosci. 81 (1), 123–137.
Hofmann, W., 2001. Late-Glacial/Holocene succession of the chironomid and cladoceran fauna of the Soppensee (Central Switzerland). J. Paleolimnol. 25 (4), 411–420.
Ilyashuk, B., Gobet, E., Heiri, O., Lotter, A.F., van Leeuwen, J.F., van der Knaap, W.O., Ilyashuk, E., Oberli, F., Ammann, B., 2009. Lateglacial environmental and climatic changes at the Maloja Pass, Central Swiss Alps, as recorded by chironomids and pollen. Quat. Sci. Rev. 28 (13–14), 1340–1353.
Ivy-Ochs, S., Schäfer, J., Kubik, P.W., Synal, H.A., Schlüchter, C., 2004. Timing of deglaciation on the northern Alpine foreland (Switzerland). Eclogae Geol. Helv. 97 (1), 47–55.
Ivy-Ochs, S., Kerschner, H., Reuther, A., Preusser, F., Heine, K., Maisch, M., Kubik, P.W., Schlüchter, C., 2008. Chronology of the last glacial cycle in the European Alps. Quat. Sci. Rev. 23, 559–573.
Johnsen, S.J., Dahl-Jensen, D., Gundestrup, N., Steffensen, J.P., Clausen, H.B., Miller, H., Masson-Delmotte, V., Sveinbjörnsdottir, A.E., White, J., 2001. Oxygen isotope and palaeotemperature records from six Greenland ice-core stations: Camp Century, Dye-3, GRIP, GISP2, Renland and NorthGRIP. Quat. Sci. Rev. 16 (4), 299–307.
Juggins, S., 2007. C2: Software for Ecological and Palaeoecological Data Analysis and Visualisation (User Guide Version 1.5). Newcastle University, Newcastle upon Tyne, p. 77.
Juggins, S., 2017. Rioja: Analysis of Quaternary Science Data. R package version (0.9-21). http://cran.r-project.org/package=rioja.
Kaltenrieder, P., Belis, C.A., Hofstetter, S., Ammann, B., Ravazzi, C., Tinner, W., 2009. Environmental and climatic conditions at a potential Glacial refugial site of tree species near the Southern Alpine glaciers. New insights from multiproxy sedimentary studies at Lago della Costa (Euganean Hills, Northeastern Italy). Quat. Sci. Rev. 28 (25–26), 2647–2662.
Kerschner, H., Ivy-Ochs, S., 2008. Palaeoclimate from glaciers: examples from the eastern Alps during the alpine lateglacial and early Holocene. Global Planet. Change 60, 58–71.
Landolt, E., 2003. Unsere Alpenflora. Gustav Fisher, Stuttgart, Germany.
Larocque, I., Finsinger, W., 2008. Late-glacial chironomid-based temperature reconstructions for Lago Piccolo di Avigliana in the southwestern Alps (Italy). Palaeogeogr. Palaeoclimatol. Palaeoecol. 257 (1–2), 207–223.
Larocque-Tobler, I., 2010. Reconstructing temperature at Egelsee, Switzerland, using North American and Swedish chironomid transfer functions: potential and pitfalls. J. Paleolimnol. 44 (1), 243–251.
Lepš, J., Šmilauer, P., 2003. Multivariate Analysis of Ecological Data Using CANOCO. Cambridge university press.
Liu, Z., Otto-Bliesner, B.L., He, F., Brady, E.C., Tomas, R., Clark, P.U., Carlson, A.E., Lynch-Stieglitz, J., Curry, W., Brook, E., Erickson, D., 2009. Transient simulation of last deglaciation with a new mechanism for Bølling-Allerød warming. Science 325 (5938), 310–314.
Lotter, A.F., Eicher, U., Siegenthaler, U., Birks, H.J.B., 1992. Late-glacial climatic oscillations as recorded in Swiss lake sediments. J. Quat. Sci. 7 (3), 187–204.
Lotter, A.F., 1999. Late-glacial and Holocene vegetation history and dynamics as shown by pollen and plant macrofossil analyses in annually laminated sediments from Soppensee, central Switzerland. Veg. Hist. Archaeobotany 8 (3), 165–184.
Lotter, A.F., Zbinden, H., 1989. Late-Glacial pollen analysis, oxygen-isotope record, and radiocarbon stratigraphy from Rotsee (Lucerne), Central Swiss Plateau. Eclogae Geol. Helv. 82 (1), 191–202.
Lotter, A.F., Heiri, O., Brooks, S., van Leeuwen, J.F., Eicher, U., Ammann, B., 2012. Rapid summer temperature changes during Termination 1a: high-resolution multi-proxy climate reconstructions from Gerzensee (Switzerland). Quat. Sci. Rev. 36, 103–113.
Luetscher, M., Boch, R., Sodemann, H., Spötl, C., Cheng, H., Edwards, R.L., Frisia, S., Hof, F., Müller, W., 2015. north Atlantic storm track changes during the last glacial maximum recorded by alpine speleothems. Nat. Commun. 6, 6344.
Ludwig, P., Pinto, J.G., Raible, C.C., Shao, Y., 2017. Impacts of surface boundary conditions on regional climate model simulations of European climate during the Last Glacial Maximum. Geophys. Res. Lett. 44 (10), 5086–5095.
Magny, M., Aalbersberg, G., Bégeot, C., Benoit-Ruffaldi, P., Bossuet, G., Disnar, J.R., Heiri, O., Laggoun-Defarge, F., Mazier, F., Millet, L., Peyron, O., 2006. Environmental and climatic changes in the Jura mountains (eastern France) during the Lateglacial–Holocene transition: a multi-proxy record from Lake Lautrey. Quat. Sci. Rev. 25 (5–6), 414–445.
Marcott, S.A., Bauska, T.K., Buizert, C., Steig, E.J., Rosen, J.L., Cuffey, K.M., Fudge, T.J., Severinghaus, J.P., Ahn, J., Kalk, M.L., McConnell, J.R., 2014. Centennial-scale changes in the global carbon cycle during the last deglaciation. Nature 514 (7524), 616–619.
Martínez-García, B., Rodríguez-Lázaro, J., Pascual, A., Mendicoa, J., 2015. The "Northern guests" and other palaeoclimatic ostracod proxies in the late Quaternary of the Basque Basin (S Bay of Biscay). Palaeogeogr. Palaeoclimatol. Palaeoecol. 419, 100–114.
McManus, J.F., Francois, R., Gherardi, J.M., Keigwin, L.D., Brown-Leger, S., 2004. Collapse and rapid resumption of Atlantic meridional circulation linked to deglacial climate changes. Nature 428 (6985), 834–837.
MeteoSwiss, 2020. Klimadiagramme und Normwerte pro Station. Federal Office of Meteorology and Climatology MeteoSwiss, Zurich-Airport, Switzerland.
Millet, L., Rius, D., Galop, D., Heiri, O., Brooks, S.J., 2012. Chironomid-based reconstruction of Lateglacial summer temperatures from the Ech palaeolake record (French western Pyrenees). Palaeogeogr. Palaeoclimatol. Palaeoecol. 315, 86–99.
Mojtahid, M., Toucanne, S., Fentimen, R., Barras, C., Le Houedec, S., Soulet, G., Bourillet, J.F., Michel, E., 2017. Changes in northeast Atlantic hydrology during Termination 1: insights from Celtic margin's benthic foraminifera. Quat. Sci. Rev. 175, 45–59.
Müller-Beck, H., 2005. Seeberg, Burgäschisee-Süd: Bauten und Siedlungsgeschichte. Acta Bernensia II, Teil 2. Stämpfli, Bern.
NAIS Divide Members, 2013. Onset of deglacial warming in West Antarctica driven by local orbital forcing. Nature 500 (7463), 440–444.
National Centre for Climate Services, 2018. In: CH2018 - Klimaszenarien für die Schweiz. National Centre for Climate Services, Zürich, 24 S.
Oksanen, J., Kindt, R., Legendre, P., O'Hara, B., Stevens, M.H.H., Oksanen, M.J., Suggests, M.A.S.S., 2007. The vegan package. Community Ecol. Package 10, 631–637.
Petit, J.R., Jouzel, J., Raynaud, D., Barkov, N.I., Barnola, J.M., Basile, I., Bender, M., Chappellaz, J., Davis, M., Delaygue, G., Delmotte, M., 1999. Climate and atmospheric history of the past 420,000 years from the Vostok ice core, Antarctica. Nature 399 (6735), 429–436.
Pons, A., Reille, M., 1988. The Holocene-and upper Pleistocene pollen record from Padul (Granada, Spain): a new study. Palaeogeogr. Palaeoclimatol. Palaeoecol. 66 (3–4), 243–263.
Quinlan, R., Smol, J.P., 2001. Setting minimum head capsule abundance and taxa deletion criteria in chironomid-based inference models. J. Paleolimnol. 26 (3), 327–342.

Quinlan, R., Smol, J.P., 2010. Use of subfossil Chaoborus mandibles in models for inferring past hypolimnetic oxygen. J. Paleolimnol. 44 (1), 43–50.
RStudio Team, 2015. RStudio. Integrated Development for R. RStudio, Inc., Boston, MA. http://www.rstudio.com/.
van Raden, U.J., Colombaroli, D., Gilli, A., Schwander, J., Bernasconi, S.M., van Leeuwen, J., Leuenberger, M., Eicher, U., 2013. High-resolution late-glacial chronology for the Gerzensee lake record (Switzerland): δ18O correlation between a Gerzensee-stack and NGRIP. Palaeogeogr. Palaeoclimatol. Palaeoecol. 391, 13–24.
Rasmussen, S.O., Andersen, K.K., Svensson, A.M., Steffensen, J.P., Vinther, B.M., Clausen, H.B., Siggaard-Andersen, M.L., Johnsen, S.J., Larsen, L.B., Dahl-Jensen, D., Bigler, M., 2006. A new Greenland ice core chronology for the last glacial termination. J. Geophys. Res. Atmos. 111 (D6).
Rasmussen, S.O., Bigler, M., Blockley, S.P., Blunier, T., Buchardt, S.L., Clausen, H.B., Cvijanovic, I., Dahl-Jensen, D., Johnsen, S.J., Fischer, H., Gkinis, V., 2014. A stratigraphic framework for abrupt climatic changes during the Last Glacial period based on three synchronized Greenland ice-core records: refining and extending the INTIMATE event stratigraphy. Quat. Sci. Rev. 106, 14–28.
Rey, F., Gobet, E., van Leeuwen, J.F., Gilli, A., van Raden, U.J., Hafner, A., Wey, O., Rhiner, J., Schmocker, D., Zünd, J., Tinner, W., 2017. Vegetational and agricultural dynamics at Burgäschisee (Swiss Plateau) recorded for 18,700 years by multi-proxy evidence from partly varved sediments. Veg. Hist. Archaeobotany 26 (6), 571–586.
Rey, F., Gobet, E., Schwörer, C., Hafner, A., Szidat, S., Tinner, W., 2020. Climate impacts on vegetation and fire dynamics since the last deglaciation at Moossee (Switzerland). Clim. Past. 16, 1347–1367. https://doi.org/10.5194/cp-16-1347-2020.
Reimer, P.J., Bard, E., Bayliss, A., Beck, J.W., Blackwell, P.G., Bronk Ramsey, C., Buck, C.E., Cheng, H., Edwards, R.L., Friedrich, M., Grootes, P.M., Guilderson, T.P., Haflidason, H., Hajdas, I., Hatté, C., Heaton, T.J., Hoffmann, D.L., Hogg, A.G., Hughen, K.A., Kaiser, K.F., Kromer, B., Manning, S.W., Niu, M., Reimer, R.W., Richards, D.A., Scott, E.M., Southon, J.R., Staff, R.A., Turney, C.S.M., van der Plicht, J., 2013. IntCal13 and Marine13 radiocarbon age calibration curves 0–50,000 years cal BP. Radiocarbon 55, 87–1869. https://doi.org/10.2458/azu_js_rc.55.16947.
Samartin, S., Heiri, O., Lotter, A.F., Tinner, W., 2012. Climate warming and vegetation response after Heinrich event 1 (16 700–16 000 cal yr BP) in Europe south of the Alps. Clim. Past 8 (6), 1913–1927.
Samartin, S., Heiri, O., Joos, F., Renssen, H., Franke, J., Brönnimann, S., Tinner, W., 2017. Warm Mediterranean mid-Holocene summers inferred from fossil midge assemblages. Nat. Geosci. 10 (3), 207–212.
Schilt, A., Baumgartner, M., Schwander, J., Buiron, D., Capron, E., Chappellaz, J., Loulergue, L., Schüpbach, S., Spahni, R., Fischer, H., Stocker, T.F., 2010. Atmospheric nitrous oxide during the last 140,000 years. Earth Planet Sci. Lett. 300 (1–2), 33–43.
Schmid, P.E., 1993. A key to the Larval Chironomidae and their instars from Austrian Danube region streams and rivers: with particular reference to a numerical taxonomic approach. 1. Diamesinae, Prodiamesinae and Orthocladiinae. Selbstverl.
Solhøy, I.W., Solhøy, T., 2000. The fossil oribatid mite fauna (Acari: Oribatida) in late-glacial and early-Holocene sediments in Kråkenes Lake, western Norway. J. Paleolimnol. 23 (1), 35–47.
Stern, J.V., Lisiecki, L.E., 2013. North Atlantic circulation and reservoir age changes over the past 41,000 years. Geophys. Res. Lett. 40 (14), 3693–3697.
Stuiver, M., Reimer, P.J., 1993. Extended 14 C data base and revised CALIB 3.0 14 C age calibration program. Radiocarbon 35 (1), 215–230.
Szadziewski, R., Krzywinski, J., Gilka, W., 1997. Diptera Ceratopogonidae, Biting Midges, 2, pp. 243–263. The aquatic insects of North Europe.
Tinner, W., 2007. Plant Macrofossil Methods and Studies/Treeline Studies.
Tinner, W., Vescovi, E., 2005. Ecologia e oscillazioni del limite degli alberi nelle Alpi dal Pleniglaciale al presente. In: Frisia, Silvia, Filippi, Maria Letizia, Borsato, Andrea (Eds.), Cambiamenti climatici e ambientali in Trentino: dal passato prospettive per il futuro. Studi Trent. Sci. Nat., Acta. Geol., vol. 82, pp. 7–14.
Tóth, M., Magyari, E.K., Buczkó, K., Braun, M., Panagiotopoulos, K., Heiri, O., 2015. Chironomid-inferred Holocene temperature changes in the south Carpathians (Romania). Holocene 25 (4), 569–582.
Tzedakis, P.C., Lawson, I.T., Frogley, M.R., Hewitt, G.M., Preece, R.C., 2002. Buffered tree population changes in a Quaternary refugium: evolutionary implications. Science 297 (5589), 2044–2047.
Ursenbacher, S., Stötter, T., Heiri, O., 2020. Chitinous aquatic invertebrate assemblages in Quaternary lake sediments as indicators of past deep-water oxygen concentration. Quat. Sci. Rev. S0277-3791(19)30950-30953.
Velle, G., Brodersen, K.P., Birks, H.J.B., Willassen, E., 2010. Midges as quantitative temperature indicator species: lessons for palaeoecology. Holocene 20 (6), 989–1002.
Verbruggen, F., Heiri, O., Meriläinen, J.J., Lotter, A.F., 2011. Subfossil chironomid assemblages in deep, stratified European lakes: relationships with temperature, trophic state and oxygen. Freshw. Biol. 56 (3), 407–423.
WAIS Divide Project Members, 2013. Onset of deglacial warming in West Antarctica driven by local orbital forcing. Nature 500 (7463), 440–444.
Watson, J.E., Brooks, S.J., Whitehouse, N.J., Reimer, P.J., Birks, H.J.B., Turney, C., 2010. Chironomid-inferred late-glacial summer air temperatures from Lough Nadourcan, Co. Donegal, Ireland. J. Quat. Sci. 25 (8), 1200–1210.
Watts, W.A., Allen, J.R.M., Huntley, B., 1996. Vegetation history and palaeoclimate of the last glacial period at Lago Grande di Monticchio, southern Italy. Quat. Sci. Rev. 15 (2–3), 133–153.
Wehrli, M., Tinner, W., Ammann, B., 2007. 16 000 years of vegetation and settlement history from Egelsee (Menzingen, central Switzerland). Holocene 17 (6), 747–761.
Chironomidae of the Holarctic region: keys and diagnoses: larvae. In: Wiederholm (Ed.), Scandinavian Soc. Entomol.